

 Open access • Posted Content • DOI:10.1101/729657

Leptin resistance establishment in the ovary of diet-induced obese mice and its relationship with cumulus cells transcriptome — Source link

Karolina Wołodko, Edyta Walewska, Juan Castillo-Fernandez, Gavin Kelsey ...+3 more authors

Institutions: Babraham Institute, University of Cambridge

Published on: 15 Aug 2019 - bioRxiv (Cold Spring Harbor Laboratory)

Topics: Diet-induced obese, Leptin, Lipotoxicity, Transcriptome and SOCS3

Related papers:

- [Leptin Resistance in the Ovary of Obese Mice Is Associated with Profound Changes in the Transcriptome of Cumulus Cells](#)
- [Role of the tumour suppressor pathway p53-p21 in the regulation of metabolism](#)
- [Renal Metabolic Programming Is Linked to the Dynamic Regulation of a Leptin-Klf15 Axis and Akt/AMPK \$\alpha\$ Signaling in Male Offspring of Obese Dams.](#)
- [Effect of high-fat diet-induced obesity on the Akt/FoxO/Smad signaling pathway and the follicular development of the mouse ovary](#)
- [Leptin resistance of adipocytes in obesity: role of suppressors of cytokine signaling.](#)

Share this paper:    

View more about this paper here: <https://typeset.io/papers/leptin-resistance-establishment-in-the-ovary-of-diet-induced-2ryqntmyn>

1 **Leptin Resistance in the Ovary of Obese Mice Is Associated with Profound**
2 **Changes in the Transcriptome of Cumulus Cells**

3

4 Karolina Wołodko¹, Edyta Walewska¹, Marek Adamowski¹, Juan Castillo-Fernandez²,
5 Gavin Kelsey^{2,3,*}, António Galvão^{1,2,3,*}

6 ¹ *Institute of Animal Reproduction and Food Research of PAS, Department of*
7 *Reproductive Immunology and Pathology, Olsztyn, Poland;*

8 ² *Babraham Institute, Epigenetics Programme, Cambridge, CB22 3AT, UK;*

9

10 ³ *University of Cambridge, Centre for Trophoblast Research, Cambridge, CB2 3EG,*
11 *UK.*

12

13 This article was first published as a preprint: Wolodko et al (2019). bioRxiv.

14 <https://doi.org/10.1101/729657>

15

16 Short title: Obesity-induced leptin resistance results in altered transcription in cumulus
17 cells

18

19 ***Corresponding authors:**

20 António Galvão

21 Antonio.Galvao@babraham.ac.uk

22 *Epigenetics Programme, Babraham Institute, Cambridge, CB22 3AT, UK*

23 a.galvao@pan.olsztyn.pl

24 *Institute of Animal Reproduction and Food Research of PAS, Olsztyn, Tuwima 10, 10-*
25 *748 Poland*

26

27 Gavin Kelsey

28 Gavin.Kelsey@babraham.ac.uk

29 *Epigenetics Programme, Babraham Institute, Cambridge, CB22 3AT, UK*

30

31

32 **Keywords:** obesity, cumulus cell, leptin, SOCS3, transcriptome

33

34 **ABSTRACT**

35 **Background/Aims:** Obesity is associated with infertility, decreased ovarian
36 performance and lipotoxicity. However, little is known about the aetiology of these
37 reproductive impairments. Here, we hypothesise that the majority of changes in ovarian
38 physiology in diet-induced obesity (DIO) are a consequence of transcriptional changes
39 downstream of altered leptin signalling. Therefore, we investigated the extent to which
40 leptin signalling is altered in the ovary upon obesity with particular emphasis on effects
41 on cumulus cells (CCs), the intimate functional companions of the oocyte. Furthermore,
42 we used the pharmacological hyperleptinemic (LEPT) mouse model to compare
43 transcriptional profiles to DIO. **Methods:** Mice were subjected to DIO for 4 and 16
44 weeks (wk) and leptin treatment for 16 days, to study effects in the ovary in components
45 of leptin signalling at the transcript and protein levels, using Western blot, Real-time
46 PCR and immunostaining. Furthermore, we used low-cell RNA sequencing to
47 characterise changes in the transcriptome of CCs in these models. **Results:** In the DIO
48 model, obesity led to establishment of ovarian leptin resistance after 16 wk high fat diet
49 (HFD), as evidenced by increases in the feedback regulator suppressor of cytokine
50 signalling 3 (SOCS3) and decreases in the positive effectors phosphorylation of tyrosine
51 985 of leptin receptor (ObRb-pTyr985) and Janus kinase 2 (pJAK2). Transcriptome
52 analysis of the CCs revealed a complex response to DIO, with large numbers and
53 distinct sets of genes deregulated at early and late stages of obesity; in addition, there
54 was a striking correlation between body weight and global transcriptome profile of CCs.
55 Further analysis indicated that the transcriptome profile in 4 wk HFD CCs resembled
56 that of LEPT CCs, in the upregulation of cellular trafficking and impairment in
57 cytoskeleton organisation. Conversely, after 16 wk HFD CCs showed expression
58 changes indicative of augmented inflammatory responses, cell morphogenesis, and
59 decreased metabolism and transport, mainly as a consequence of the physiological
60 changes of obesity. **Conclusion:** Obesity leads to ovarian leptin resistance and major
61 time-dependent changes in gene expression in CCs, which in early obesity may be
62 caused by increased leptin signalling in the ovary, whereas in late obesity are likely to
63 be a consequence of metabolic changes taking place in the obese mother.

64

65

66 INTRODUCTION

67 Obesity is considered one of the major public health challenges of modern times and
68 has been linked to various comorbidities, such as metabolic syndrome, type 2 diabetes,
69 cancer, stroke (1) and infertility (2). Obese women have increased risk of menstrual
70 dysfunctions and anovulation, pregnancy complications, and poor reproductive outcome
71 (3). In mouse models, obesity is characterised by lipid accumulation in the ovary and
72 ensuing lipotoxicity (4) and oxidative stress (5). Nonetheless, the exact mechanisms
73 underlying ovarian pathogenesis in the course of obesity remain uncharacterised.

74 Leptin is a cytokine secreted by the adipose tissue (adipokine) (6). Indeed, soon
75 after the introduction to an obesogenic environment, large amounts of leptin can be
76 found in the circulation (7), making this adipokine one of the early-onset obesity
77 markers. Leptin controls food intake through its action at the central nervous system (8);
78 however, as a pleiotropic adipokine, leptin contributes to the regulation of numerous
79 processes in the body, such as immune response (9) or angiogenesis (10). Concerning
80 the reproductive tract, leptin has been shown to control the neuroendocrine reproductive
81 axis (11) and folliculogenesis (12). Furthermore, leptin has been linked to ovulation
82 (13) and embryo development (14). Leptin is detected in most cell types in the murine
83 ovary, with the highest staining intensity seen in the oocyte (15). Nevertheless, no
84 previous consideration has been made whether leptin signalling is dysregulated in the
85 obese ovary. The leptin receptor b (ObRb) is a type I cytokine receptor, which signals
86 through the association with the tyrosine kinase Janus kinase 2 (JAK2). Upon leptin
87 binding and dimerization of the receptor, JAK2 is recruited (16), mediating the
88 phosphorylation of three conserved tyrosine residues on the intracellular domain of the
89 receptor: tyrosine (Tyr) 985, Tyr1077 and Tyr1138. Subsequently, signalling molecules
90 are recruited to these activated tyrosines (17) and, as a result, the signal transducer and
91 activator of transcription (STAT) 5 and/or STAT3 are also phosphorylated and
92 translocated into the nucleus, where they regulate transcription (8,18). During sustained
93 activation of ObRb, the expression of both suppressor of cytokine signalling 3 (SOCS3)
94 and tyrosine-protein phosphatase 1B (PTP1B) is initiated as a negative feedback
95 response (19,20). While PTP1B dephosphorylates JAK2, SOCS3 binds to receptor
96 domains within JAK2 and Tyr985 and terminates signal transduction.

97 To date, little is known about the integrity of leptin signalling in the ovary
98 during obesity progression, and its particular impact on the cumulus oophorous complex
99 (COC). Cumulus cells (CCs) are vital regulators of oocyte growth and metabolism (21),
100 controlling meiosis resumption (22), as well as the ovulation process itself (23). Thus, a

101 better knowledge of the pathophysiology of the events taking place in these cells in the
102 course of obesity will allow us to understand the molecular mechanisms leading to
103 impaired ovarian performance and infertility. Furthermore, the transcriptional signature
104 of CCs has been used to predict oocyte competence or embryo quality (24,25),
105 demonstrating the importance of such references in assisted reproduction techniques.
106 Here, we first characterise the establishment of leptin resistance in whole ovaries from
107 diet induced obesity (DIO) mice fed for 4 and 16 weeks (wk). Subsequently, we
108 analysed the transcriptome of CCs throughout obesity progression and identify
109 temporally altered gene expression signatures. Finally, using a mouse model for
110 pharmacological hyperleptinemia (LEPT), we pinpoint the transcriptional events
111 mediated by increased leptin signalling in CCs in the early stages of obesity.

112

113 **MATERIALS AND METHODS**

114 *Animal protocol*

115 Breeding pairs from mouse strains C57BL/6J (B6) and B6.Cg-Lep^{ob}/J (*ob/ob*) were
116 obtained from the Jacksons Laboratory (The Jacksons Laboratory, Bar Harbour, Maine,
117 USA). At 8 wk of age B6 animals were divided into 2 groups (n=12/ group). In DIO,
118 the control group was fed *ad libitum* chow diet (CD, 11% energy in kcal from fat, 5053,
119 rodent diet 20, LabDiet IPS, London, UK), while the experimental group received high
120 fat diet (HFD, 58% energy in kcal from fat, AIN-76A 9G03, LabDiet IPS). Mice were
121 maintained on the respective diet for 4 or 16 wk. Regarding the pharmacological
122 hyperleptinemia protocol, 8 wk old B6 female mice fed CD were divided into two
123 groups (n=15/group): i) saline 16 days (d) (CONT); ii) leptin 16 d (Recombinant Mouse
124 Leptin, GFM26, Cell Guidance Systems, Cambridge, UK). The animals were injected
125 intraperitoneally twice a day, at 09:00 h and 21:00 h and total dosage of 100 µg/day of
126 leptin was administrated. Concerning the *ob/ob* model, mice were kept from weaning
127 until twelve wk of age on CD. For all protocols, mice were housed with a 12 h light/12
128 h dark cycle at room temperature (23°C, RT).

129 For phenotype characterisation of DIO, changes in body composition were
130 monitored every 4 wk by nuclear magnetic resonance (NMR, Bruker, Rheinstetten,
131 Germany), whereas in the LEPT model animals were phenotyped every three days.
132 Body weight (BW), fat mass (FM), lean mass (LM), adiposity index (AI, fat mass/lean
133 mass), and food intake (FI) were measured. For DIO and LEPT models vaginal
134 cytology was done at 9:00 h, for twelve consecutive days. After vaginal lavage with
135 saline, the smears were placed on clean glass slides and stained with Diff Quick

136 Staining Set (Diff- Quick Color Kit, Rapid Staining Set, Medion Grifols Diagnostics
137 AG, Duedingen, Switzerland), for cell identification as previously described (26). The
138 results were analysed for percent of time spent in oestrous stage (further explained in
139 Figure supplement 1J, 1K; Figure supplement 6G). All samples for mRNA, protein
140 analysis and staining were collected at the oestrus stage.

141 A superovulation protocol was used for COC collection and further isolation of a
142 pure population of CCs after removing the metaphase II (MII) oocytes. This
143 developmental state of granulosa cells (GC) was preferred to ensure a tightly controlled
144 level of progression. The animals were injected with pregnant mare's serum
145 gonadotropin (PMSG, G4877, 5IU, Sigma Aldrich, Saint Louis, Missouri, USA)
146 followed after 48 h by human chorionic gonadotropin (hCG, Chorulon, 5IU, MSD
147 Animal Health, Boxmeer, Holland). Subsequently, 18 h after hCG injection the animals
148 were sacrificed.

149

150 *Ovary collections*

151 Mice were sacrificed by cervical dislocation and the reproductive tracts collected and
152 rinsed with phosphate buffered saline (PBS, 0.1M, pH=7.4). Ovaries were then removed
153 from the genitalia and cleaned of adipose tissue. Ovaries were stored either in TRI
154 Reagent (T9424, Sigma Aldrich) for mRNA, or radioimmunoprecipitation assay buffer
155 (RIPA, 89901, ThermoFisher Scientific, Waltham, Massachusetts, USA) supplemented
156 with protease inhibitor cocktail (PIC, P8340, Sigma Aldrich), phenylmethylsulfonyl
157 fluoride (PMSF, P7626, Sigma Aldrich) and phosphatase inhibitor (88667, Thermo
158 Fisher Scientific), for protein analysis. Samples were stored in -80°C, except for the
159 analysis of phosphorylated proteins, in which samples were isolated immediately after
160 sacrificing the animals.

161

162 *Ovarian cell isolation protocol*

163 For theca and stroma enriched (TC) fraction collection, immediately after culling the
164 animals, ovaries were transferred to Dulbecco's modified Eagle's medium (DMEM,
165 D/F medium; 1:1 (v/v), D-8900, Sigma Aldrich) with 3% bovine serum albumin (BSA,
166 735078, Roche Diagnostics GmbH, Mannheim, Germany), 20 µg/ml gentamicin
167 (G1397, Sigma Aldrich) and 250 µg/ml amphotericin (A2942, Sigma Aldrich). For the
168 TC fraction, ovaries were punctured with a 16 gauge needle as described before (27).
169 Briefly, after removing GC and oocytes, the remaining tissue was washed twice with
170 media and stored in TRI Reagent for mRNA analysis (n=8/group). For CCs, after

171 superovulating the animals, COCs were retrieved from oviducts, and further digested
172 with hyaluronidase (H3506, 400 µg/ml, Sigma Aldrich). After removing the oocytes, a
173 total of approximately 50 pure CCs were collected from one individual animal from
174 either 4 wk or 16 wk DIO (n=5/ condition), as well as the 16 d LEPT (n=at least 3/
175 condition) protocol.

176

177 *RNA isolation and cDNA synthesis*

178 For mRNA extraction, either whole ovaries or TC fraction were collected from mice in
179 oestrus stage, placed in 1 ml of TRI Reagent in 1.5 ml eppendorf tubes (n=8/ group) and
180 mechanically disrupted with a lancet. The suspension was pipetted up and down
181 vigorously and incubated for 5 minutes (min) at RT. After centrifugation (9400 g, 4□,
182 15 min), the supernatant was transferred to a fresh tube and thoroughly mixed with 100
183 µl of 1-Bromo-3-chloropropan (BCP, BP151, Molecular Research Centre, Cincinnati,
184 Ohio, USA), followed by incubation at RT for 10 min. Subsequently, samples were
185 centrifuged (13500 g, 4□, 15 min) and the aqueous phase transferred to a new tube,
186 before being mixed with an equal volume of isopropanol and incubated at -80°C for 60
187 min. Another centrifugation (20000 g, 4□, 15 min) to pellet down the RNA, which was
188 then washed three times with 75% ethanol and incubated overnight in -80°C. Next day,
189 samples were centrifuged (20000 g, 4□, 15 min) and the RNA pellet dried and
190 resuspended in 20 µl of RNase free water (W4502, Sigma Aldrich), supplemented with
191 RNase Inhibitor (RiboProtect, RT35, BLIRT, Gdańsk, Poland). Finally, RNA quality
192 and concentration were assessed with NanoDrop. Absorbance ratio at 260 nm and 280
193 nm (A260/A280) was determined and the quality and concentration of isolated mRNA
194 confirmed.

195 A total of 1 µg of RNA was reversely transcribed using Maxima First Strand
196 cDNA Synthesis Kit for Real-time polymerase chain reaction (PCR) (K1642,
197 ThermoScientific) according to the manufacturer's instructions. The cDNA was stored
198 in -20°C until the real-time PCR was carried out.

199

200 *Real-time polymerase chain reaction*

201 Real-time PCR was performed in a 7900 Real-Time PCR System (Applied Biosystems,
202 Warrington, UK) using Maxima SYBR Green/ROX qPCR Master Mix (K0223,
203 ThermoScientific). Primers were designed using Primer 3.0 v.0.4.0. software (28),
204 based on gene sequences from GeneBank (NCBI), as described before (29). All primers
205 were synthesised by Sigma Aldrich. Primer sequences, expected PCR products length,

206 and GeneBank accession numbers are reported in Table 1. The total reaction volume
207 was 12 μ l, containing 4 μ l cDNA (10 μ g), 1 μ l each forward and reverse primers (80 nM
208 or 160 nM), and 6 μ l SYBR Green PCR master mix. Real-time PCR was carried out as
209 follows: initial denaturation (10 min at 95 $^{\circ}$ C), followed by 45 cycles of denaturation (15
210 s at 95 $^{\circ}$ C) and annealing (1 min at 60 $^{\circ}$ C). After each PCR, melting curves were obtained
211 by stepwise increases in temperature from 60 to 95 $^{\circ}$ C to ensure single product
212 amplification. In each real-time assay, both the target gene and a housekeeping gene
213 (HKG) - *Ribosomal Protein L37 (Rpl37*, primers in Table 1) or *Eukaryotic Translation*
214 *Initiation Factor 5A (Eif5a*, primers in Table 1) - were run simultaneously and reactions
215 were carried out in duplicate wells in a 384-well optical reaction plate (4306737,
216 Applied Biosystems). The HKG selection was performed with NormFinder, in each
217 experimental group. Real-time PCR results were analysed with the Real-time PCR
218 Miner algorithm (30).

219

220 *Western blot*

221 Protein expression was assessed by western blot (n=5/group). Ovaries from mice in
222 oestrus stage were collected into RIPA supplemented with inhibitors and mechanically
223 disrupted with a lancet. Then, lysates were incubated for one hour on ice, with mixing
224 every 15 min. Subsequently, samples were centrifuged (20000 g, 4 $^{\circ}$ C, 15min) and the
225 supernatant was collected and stored in -80 $^{\circ}$ C until the analysis. The protein
226 concentration was assessed using bicinchoninic acid assay (BCA, BCA1-1KT, Sigma
227 Aldrich). A total of 10-40 μ g of protein was loaded on 8-14% acrylamide gel, and after
228 electrophoresis proteins were transferred to polyvinylidene difluoride (PVDF) or
229 nitrocellulose membrane depending on the antibodies to be used. Membranes were
230 blocked in 5% BSA (A2153, Sigma Aldrich) and incubated with primary antibodies
231 (AB) overnight at 4 $^{\circ}$ C. Leptin receptor and its phosphorylated domains were evaluated
232 using the following antibodies: mouse monoclonal (MM) against leptin receptor (ObR;
233 1:500, cat# sc-8391, Santa Cruz Biotechnology, Dallas, Texas, USA), goat polyclonal
234 (GP) against phosphorylated Tyr 985 ObRb (pTyr985ObRb; 1:500, cat# sc-16419,
235 Santa Cruz Biotechnology), rabbit polyclonal (RP) against phosphorylated Tyr 1077
236 ObRb (pTyr1077ObR; 1:500, cat# 07-1317, Merck Millipore, Burlington, Vermont,
237 USA), GP against phosphorylated Tyr 1138 ObRb (pTyr1138ObRb; 1:500, cat# sc-
238 16421, Santa Cruz Biotechnology). The expression of other leptin signalling pathway
239 components was assessed using the following antibodies: RP against JAK2 (1:200, cat#
240 sc-294, Santa Cruz Biotechnology), RP against phosphorylated Tyr 1007/1008 JAK2

241 (pJAK2; 1:200, cat# sc-16566-R, Santa Cruz Biotechnology), RP against STAT3 (1:200,
242 cat# sc-482, Santa Cruz Biotechnology), MM against phosphorylated Tyr 705 pSTAT3
243 (1:200, cat# sc-8059, Santa Cruz Biotechnology), RP against STAT5 (1:200, cat# sc-
244 835, Santa Cruz Biotechnology), MM against phosphorylated Tyr 694/699 pSTAT5
245 (1:200, cat# sc-81524, Santa Cruz Biotechnology), GP against PTP1B (1:200, cat# sc-
246 1718, Santa Cruz Biotechnology), MM against SOCS3 (1:500, cat# sc-51699, Santa
247 Cruz Biotechnology) in cell lysates. The results were normalized with β -actin (1:10000,
248 MM, cat# A2228, Sigma-Aldrich). All antibodies specifications are summarised in
249 Table 2. Proteins were detected after incubation of the membranes with secondary GP
250 anti-rabbit alkaline phosphatase-conjugated antibody (1:30000, cat# A3687, Sigma
251 Aldrich), GP anti-mouse alkaline phosphatase-conjugated antibody (1:20000, cat#
252 31321, ThermoScientific), RP anti-goat alkaline phosphatase-conjugated (1:30000, cat#
253 A4187, Sigma Aldrich), or RP anti-goat horseradish peroxidase- conjugated antibody
254 (1:75000, cat# A50-100P, Bethyl, Montgomery, Alabama, USA) for 2 h at RT. Immune
255 complexes were visualized using the alkaline phosphatase visualization procedure or
256 ECL substrate visualization. Blots were scanned in a Molecular Imager VersaDoc MP
257 4000 System (BioRad, Hercules, California, USA) and specific bands quantified using
258 ImageLab Software (BioRad). Finally, band density for each protein was normalised
259 against β -actin.

260

261 *Immunohistochemistry and immunofluorescent staining*

262 Ovaries collected from mice in oestrus stage (n=3/group) were fixed in 4% neutral
263 phosphate-buffered formalin (NBF, 432173427, Poch, Gliwice, Poland) at 4°C for 24 h,
264 and subsequently dehydrated in ethanol. Paraffin embedded ovarian tissues were
265 sectioned into 5 μ m slices. For antigen retrieval, sections were heated in citrate buffer
266 (10 mM, pH=6.0). Tissue was incubated in blocking solution (ab64261, Abcam,
267 Cambridge, UK) for 1 h at RT and primary RP anti-SOCS3 antibody (1:1000, ab16030,
268 Abcam) or primary RP anti-PTP1B antibody (1:500, ab189179, Abcam) added
269 overnight at 4°C. The negative control sections were incubated with RP anti-
270 immunoglobulin G (IgG, cat# ab37415, Abcam) or without primary antibody. The
271 primary antibody complexes were detected after incubating the tissue with biotinylated
272 goat anti-rabbit IgG (H+L) (ab64261, Abcam) for 60 min, and streptavidin peroxidase
273 for 40 min. Staining was evident after 15 s incubation in 3,3-diaminobenzidine (DAB)
274 peroxidase substrate solution (Rabbit-specific HRP/DAB (ABC) Detection IHC Kit,
275 ab64261, Abcam). Subsequently, samples were counterstained with haematoxylin

276 (MHS16, Sigma Aldrich) and mounted. Sections were examined using Axio Observer
277 Systems Z1 microscope (Carl Zeiss Microscopy GmbH, Hannover, Germany) and Zeiss
278 ZEN 2.5 lite Microscope Software (Carl Zeiss, Germany). For immunofluorescence (IF),
279 5 μ m sections were deparaffinised and rehydrated in an ethanol series. Next, tissues
280 were permeabilised in 0.3% Triton X-100 (T8787, Sigma Aldrich), followed by antigen
281 retrieval in citrate buffer (10 mM, pH=6.0) for 40 min in 90 \square and blocking in 2% BSA
282 (A2153, Sigma Aldrich) with 0,3 M glycine (G8898, Sigma Aldrich) in PBS-0.1%
283 Tween 20 (P7949, Sigma Aldrich) (PBST) solution. Sections were then incubated with
284 0.3% Sudan Black (199664, Sigma Aldrich) in 70% ethanol for 10 min at RT, followed
285 by washes in PBST. Slides were subsequently incubated with RP anti-SOCS3 antibody
286 (1:200, ab16030, Abcam) overnight at 4 \square C. The negative control sections were
287 incubated with RP anti-IgG (1:200) as before, or without primary antibody. On the next
288 day slides were washed in PBST, followed by incubation with cyanine 3 (Cy3)- donkey
289 polyclonal anti-rabbit IgG (H+L) (711-165-152, Jackson ImmunoReserach,
290 Cambridgeshire, UK), and a series of washes in PBST. Finally, slides were covered
291 with a drop of Prolong Gold medium with diamidino-2-phenylindole (DAPI) and sealed
292 with cover slips. Images were captured using 40x/1.2A or 63x/1.4A oil immersion
293 objectives on a LSM800 confocal microscope (Carl Zeiss, Germany).

294

295 *Enzyme-linked immunosorbent assay*

296 Animals in oestrus were sacrificed (n=8/group) and blood samples collected after
297 puncturing the heart. Blood samples were centrifuged (180 g, 4 \square , 10 min) and plasma
298 stored at -80 \square . Levels of circulating leptin and insulin were assessed with enzyme-
299 linked immunosorbent assay (ELISA) kit, according to the manufacturer's instructions
300 (Mouse Leptin ELISA Kit, 90030; Crystal Chem, Zaandam, Netherlands; Rat/Mouse
301 Insulin ELISA Kit, cat. EZRMI-13K; Merck Millipore). The intra- and interassay
302 coefficients of variation (CVs) were as follows: for Leptin ELISA kit <10% both and for
303 Insulin ELISA kit 8.35% and 17.9%, respectively. To determine SOCS3 in ovarian
304 extracts, ELISA test was used (ELISA KIT for SOCS3; cat no SEB684Mu, Cloud-
305 Clone, Texas, USA). Briefly, the tissue was minced in lysis buffer (n=8/group),
306 centrifuged (10000 g, 4 \square , 5 min) and protein concentration in the lysate determined with
307 BCA test. All tests and assessments were performed according to the manufacturer's
308 instructions.

309

310 *RNA-seq library generation*

311 Once the 16 wk HFD group presented divergence in BW gain, we identified 3 animals
312 with less than 33 g of body weight that we designated as HFD low gainers (HFDLG)
313 and excluded them from the regular HFD group for the further description of differently
314 expressed genes (DEGs) between CD and HFD. CCs were collected into RLT buffer
315 (1053393, Qiagen, Hilden, Germany) and kept at -80°C until library generation.
316 Subsequently, RNA sequencing (RNA-seq) libraries were prepared following a
317 previously described protocol (31,32), with minor changes. Briefly, mRNA was
318 captured using Smart-seq2 oligo-dT pre-annealed to magnetic beads (MyOne C1,
319 Invitrogen, Carlsbad, California, USA). The beads were resuspended in 10 µl of reverse
320 transcriptase mix (100 U, SuperScript II, Invitrogen; 10 U, RNAsin, Promega,
321 Madison, Wisconsin, USA), 1× Superscript II First-Strand Buffer, 2.5 mM
322 dithiothreitol (DTT, Invitrogen), 1 M betaine (Sigma Aldrich), 9 mM magnesium chloride
323 (MgCl₂, Invitrogen), 1 µM Template-Switching Oligo (Exiqon, Vedbaek, Denmark), 1
324 mM deoxyribonucleotide triphosphate (dNTP) mix (Roche) and incubated for 60 min at
325 42°C followed by 30 min at 50°C and 10 min at 60°C (31,32). Amplification of the
326 cDNA was then undertaken after adding 11 µl of 2× KAPA HiFi HotStart ReadyMix
327 and 1 µl of 2 µM ISPCR primer (31,32), followed by the cycle: 98°C for 3 min, then 9
328 cycles of 98°C for 15 s, 67°C for 20 s, 72°C for 6 min and finally 72°C for 5 min.
329 Finally, the cDNA was purified using a similar volume of AMPure beads (Beckman
330 Coulter, Brea, California, USA) and eluted into 20 µl of nuclease-free water (P1195;
331 Promega). All libraries were prepared from 100 to 200 pg of cDNA using the Nextera
332 XT Kit (Illumina, San Diego, California, USA), according to the manufacturer's
333 instructions. The final cDNA libraries were purified using a 0.7:1 volumetric ratio of
334 AMPure beads before pooling and sequencing on an Illumina Nextseq500 instrument in
335 75-base pair (bp) single-read high output mode at the Babraham Institute Sequencing
336 Facility. A total of 5-10 million mappable reads per sample were obtained, with an
337 average of 30-50 million reads per condition.

338

339 *Library mapping and trimming*

340 Trim Galore v0.4.2 was used with default parameters on raw Fastq sequence files.
341 Mapping of the RNA-seq data was done with Hisat v2.0.5 against the mouse GRCm38
342 genome, as guided by known splice sites taken from Ensemble v68.

343

344 *RNA-seq differential expression analysis*

345 Mapped RNA-seq reads were quantified and analysed using SeqMonk version v1.45.4
346 (<http://www.bioinformatics.babraham.ac.uk/projects/seqmonk/>). Differential expression
347 analysis was performed using DESeq2 (33) implemented in SeqMonk setting a false
348 discovery rate (FDR) < 0.05.

349

350 *Statistical analysis*

351 Statistical analysis was performed using GraphPad Prism 7.0. The D'Agostino-Pearson
352 omnibus normality test was performed followed by nonparametric Mann-Whitney test
353 or multiple unpaired t-test with statistical significance determined using the Bonferroni-
354 Sidak method, depending on the experiment. The data are shown as the mean \pm SD of
355 three or more independent replicates. Significance was defined as values of $p < 0.05$.

356

357 *Statement of Ethics*

358 All experiments were approved by Local Committee for the Ethical Treatment of
359 Experimental Animals of Warmia- Mazury University (Agreement No. 80/2015,
360 15/2018, 38/2018), Olsztyn, Poland and were performed accordingly to the Guide for
361 Care and Use of Laboratory Animals, endorsed by European legislation.

362

363 **RESULTS**

364 ***1. Leptin signalling is impaired in the ovary of diet-induced obese mice***

365 Initially we sought to characterise changes in leptin signalling in the ovary throughout
366 DIO. Thus, mice were subjected to HFD for 4 and 16 wk and whole ovaries and TC
367 fraction were collected for mRNA or protein analysis (Figure 1A). Oestrous stage was
368 followed for twelve consecutive days, confirming that samples were collected in oestrus
369 (Figure supplement 1J, 1K) in cycling animals. Mice significantly gained BW and FM
370 already at 4 wk, with an average absolute gain in BW of 13 grams (g) in the 16 wk HFD
371 group (Figure supplement 1A; $p < 0.0001$). Three animals with comparable FI but BW
372 gain less than 13 g were excluded from the statistical analysis and designated as HFD-
373 low gainers (HFDLG). Also, after 4 and 16 wk HFD we confirmed high plasma levels
374 of insulin (Figure supplement 1F; $p < 0.01$, $p < 0.001$ respectively) and leptin (Figure
375 supplement 1G; $p < 0.01$, $p < 0.001$ respectively) and the establishment of impaired
376 glucose tolerance and insulin resistance at 16 wk HFD (Figure supplement 1H, 1I;
377 $p < 0.01$, $p < 0.001$ respectively). Monitoring oestrous cycle revealed that the 4 wk HFD
378 group had higher prevalence of oestrus counts compared with controls fed CD, whereas

379 in the 16 wk HFD group there was a reduction in pro-oestrus (Figure supplement 1J,
380 1K; $p < 0.05$, $p < 0.01$ respectively).

381 Next, we isolated protein from whole ovaries and studied the abundance of
382 components of the leptin signalling pathway. Whilst we found initial hyperactivation of
383 leptin signalling pathway as demonstrated by upregulation of SOCS3 protein (Figure
384 1B; Figure Supplement 2H; $p < 0.05$ both) and a tendency to increased phosphorylation
385 of STAT3 (Figure supplement 2E; $p = 0.06$), after 16 wk HFD local leptin resistance was
386 clearly established. This was evidenced by the decrease in abundance of leptin receptor
387 (Figure supplement 2A; $p < 0.01$), and a trend towards decreased phosphorylation of
388 pTyr985 ObRb (Figure 1C; $p = 0.09$) and decreased phosphorylation of JAK2 (Figure
389 1D; $p < 0.05$), along with upregulation of SOCS3 (Figure 1B; $p < 0.001$, Figure
390 supplement 2H; $p < 0.05$). In contrast, no differences were found in phosphorylation of
391 other Tyr residues of ObRb (Figure supplement 2C and 2D) or in PTP1B expression
392 (Figure supplement 2G). Additionally, there was reduced phosphorylation of STAT5
393 after 4 and 16 wk HFD (Figure supplement 2F; both $p < 0.01$).

394 Next, we sought to characterise the extent to which various ovarian components
395 responded similarly to increased circulating leptin during obesity. We performed real-
396 time PCR analysis of whole ovaries and TC fraction. Despite no significant changes
397 after 4 wk HFD, the mRNA of *Socs3* was increased after 16 wk HFD in both whole
398 ovary (Figure 1E; $p < 0.05$) and TC (Figure 1E; $p < 0.001$), in comparison to the CD group.
399 Additionally, the mRNA level of *Ptp1b* was increased in both whole ovary and TC after
400 16 wk HFD (Figure 1E; $p < 0.01$, $p < 0.001$ respectively).

401 The aforementioned results suggested that SOCS3 could be an important player
402 in the establishment of leptin resistance in the ovary of obese mice. Therefore, we
403 examined SOCS3 localisation in ovaries of DIO and the genetically obese model: mice
404 with a mutation in the obese gene (*ob/ob*). Immunohistochemistry (IHC) revealed the
405 presence of SOCS3 protein in oocytes from follicles in all developmental stages (Figure
406 1H-K; Figure supplement 3E, 3F, 3I, 3J); in addition, theca cells and GC from the
407 respective follicles were stained, as well as the ovarian stroma (Figure 1H-K).
408 Importantly, we compared the IHC staining of SOCS3 and PTP1B in 16 wk HFD
409 ovaries, which suggested that SOCS3 is the major ObRb inhibitor being expressed in
410 the oocyte and GC, as PTP1B protein presented almost no staining in the oocyte (Figure
411 supplement 3G, 3H, 3K, 3L). As a control for the specificity of the IHC data, we used
412 confocal microscopy for immunofluorescence detection of SOCS3 on sections from
413 DIO and leptin-deficient *ob/ob* (-/-) ovaries, confirming the localisation of SOCS3

414 (Figure 1N-Q) and observing a weaker intensity of SOCS3 in both oocyte and GC in
415 ovaries from *ob/ob* (Figure supplement 3T, 3V) compared to wild type (+/+) (Figure
416 supplement 3S, 3U). These IF results confirmed the specificity of the staining, since
417 SOCS3 is expected to be less abundant in tissues from the *ob/ob* mouse (34).
418 Furthermore, we also inferred that impaired leptin signalling in the ovary is likely to
419 have direct implications for the oocyte, since the gamete was shown to express SOCS3.

420

421 ***2. Cumulus cell transcriptome analysis: global transcriptome of CCs reflects body*** 422 ***weight***

423 Next, we repeated the protocol and subjected the animals to superovulation in order to
424 collect CCs and analyse the transcriptome from 4 wk and 16 wk DIO protocols (Figure
425 2A). A total of 50-80 CCs per animal were collected, from which RNA-seq libraries
426 were generated using a Smart-seq2 oligo-dT method (31,32), with separate RNA-seq
427 libraries made from the CC from each female. We then used Principal Component
428 Analysis (PCA) to study the distribution of our samples according to global gene
429 expression profile, and found that principal component 1 (PC1) was mainly driven by
430 BW (Figure 2B). Here we decided to include the HFDLG from the 16wk HFD group as
431 a control, to test whether the transcriptional response could be linked to the BW of the
432 animals; indeed, the HFDLG samples clustered together with 16 wk CD of a similar
433 weight (Figure 2B). The correlation between PC1 and BW was $r=0.777$ ($p=3.026e-06$)
434 (Figure 2C; table 4), which substantiates the physiological effect driven by BW, rather
435 than the nature of the diet itself, on the global gene expression profile of CCs.

436 Next, we aimed to identify DEGs in CCs: for this analysis, we excluded the 3
437 HFDLG outliers from the 16wk HFD, so as to ensure a minimum of 13 g of BW
438 difference between CD 16 wk and HFD 16 wk and a BW difference of 5 g between CD
439 4 wk and HFD 4 wk (Figure Supplement 1A). After DESeq2 analysis (FDR <0.05), a
440 total of 997 DEGs in 4 wk HFD (373 upregulated and 624 downregulated; Figure 2D;
441 table 5) and 846 DEGs in 16 wk HFD (203 upregulated and 643 downregulated; Figure
442 2E table 5) were identified. Surprisingly, amongst the DEGs only 52 genes were
443 common between the 4 wk and 16 wk comparisons (Figure 2F), highlighting the
444 differences in pathophysiology of early and late stages of obesity. Gene ontology (GO)
445 (35,36) analysis of the DEG lists showed that transcripts with increased abundance in 4
446 wk HFD were primarily linked to nitrogen and lipid metabolism and transport, but also
447 cell stress and reactive oxygen species generation (Table 6). Transcripts downregulated
448 after 4 wk HFD were mapped to pathways involved in regulation of macromolecule

449 biosynthesis and gene expression, as well as chromatin organisation/histone
450 modification and regulation of cell cycle (Figure supplement 4A; Table 6). After 16 wk
451 HFD treatment, upregulated genes were associated with negative regulation of
452 development and cellular component organisation, while pathways highlighted for
453 downregulated genes included localisation, transport and positive regulation of
454 metabolism (Figure supplement 4B; Table 7). Therefore, in this analysis we identified
455 the gene signatures in CCs altered at the onset and later development of DIO.

456 Finally, we wished to examine the impact of BW as a factor on gene expression
457 in CCs. Therefore, we examined the expression of the 846 DEGs identified in 16 wk
458 HFD group in the 16 wk HFDLG and CD samples. Strikingly, for this set of genes, the
459 HFDLGs presented an expression pattern closer to 16 wk CD than to 16 wk HFD
460 (Figure 2G), revealing a very strong correlation between BW and global gene
461 expression profile in CCs indicative of the impact of female physiology on CCs gene
462 expression. As CCs represent an important accessible source of biomarkers for the
463 assessment of reproductive potential of the mother, they are often sampled in assisted
464 reproductive technologies (ART) to profile biomarkers of oocyte competence or embryo
465 quality. Thus, we looked for known markers of embryo quality (25) in the 16 wk DEGs
466 and discovered that *Nfib* was upregulated and *Ptgs2* and *Trim28* transcripts were
467 downregulated in CCs (Figure supplement 5A-C). The altered expression of these
468 markers in CCs during late obesity might indicate direct consequences for oocyte and
469 embryo quality, as previously proposed (24,37–39).

470

471 **3. Differential effects on gene expression in CCs early and late in obesity**

472 We next sought to characterise how gene expression in CCs changes between the early
473 and late stages of DIO. To do this, we first evaluated the expression of the 997 DEGs
474 from 4 wk and the 846 DEGs from 16 wk HFD at both time-points, aiming to identify
475 the directionality of gene signatures throughout obesity (Figure 3A). Note that in this
476 analysis, only a minority of the DEGs are significantly altered at both time points (as
477 noted above in figure 2F). Only 3 DEGs were upregulated in both conditions (Figure
478 3A), whereas we found 252 genes upregulated in 4 wk HFD but downregulated in 16
479 wk HFD, mainly linked to cell transport and localisation. Conversely, the 30 genes
480 downregulated in 4 wk HFD, but upregulated in 16 wk HFD referred to immune
481 response (Figure 3A). Finally, a sum of 694 DEGs were downregulated in both 4 and 16
482 wk HFD, mainly involved in metabolism and transcription (Figure 3A; Table 8). This
483 analysis revealed a large subset of genes being downregulated throughout obesity, but
484 also genes with opposite profile which suggest an adaptive response of CCs to changes

485 in the physiology of the mother. In a parallel approach, we intersected the DEGs
486 datasets from 4wk HFD and 16wk HFD and from the 52 DEGs in common between the
487 two timepoints (Figure 2F) identified 5 main clusters of differently expressed genes.
488 The first 2 clusters comprised 33 genes downregulated in both 4 wk and 16wk HFD
489 (Table 8), with the most significantly deregulated gene at 4 wk HFD *MICAL Like*
490 (*Micall*) 1 (FDR = 0.0002), but other genes like *Dynein cytoplasmic 1 heavy chain*
491 (*Dync1h*) or *Collagen (Col) 6a3* (Figure 3B; Table 8) were also found. Clusters 3 and 4
492 revealed the most interesting set of genes concerning disease progression, due to their
493 opposite profile between 4 wk and 16 wk treatment. In cluster 3 we found genes like
494 *Annexin (Anxa) 11* or *Exportin (Xpo) 5* strongly upregulated in 4 wk HFD, but inhibited
495 in 16 wk HFD (Figure 3B), whereas in cluster 4 we found genes like *Ras homology*
496 *family member U (Rhou)* with opposing profiles at the two time points (Figure 3B).
497 Finally, cluster 5 comprised the 3 genes significantly upregulated throughout obesity
498 (Figure 3B). Therefore, in this analysis we identified gene expression profiles in CCs
499 that represent a valuable tool to assess disease progression in the ovary of obese mice.

500

501 **4. The contribution of leptin to changes in gene expression in CCs from obese mice**

502 After identifying the major molecular changes in leptin signalling in the ovaries of DIO
503 females, we aimed to establish an *in vivo* system that would expose the ovaries to the
504 elevated levels of circulating leptin, a feature seen in obesity (7), but lacking all
505 remaining traits of obesity. Thus, we conceived a model for pharmacological
506 hyperleptinemia. Sixteen days of leptin treatment resulted in a consistent drop in BW
507 and FM (Figure supplement 6B, 6E; $p < 0.01$) and increased incidence of oestrus (Figure
508 supplement 6G; $p < 0.05$). The ovaries from animals in oestrus stage were collected for
509 mRNA and protein analysis. Whereas injections of 100 μg leptin for 9 days did not
510 change the protein expression of leptin signalling molecules (Figure supplement 7A-J),
511 ObR expression and phosphorylation of Tyr985 and STAT5 were decreased after 16 d
512 (Figure supplement 7A, 7B, 7G; $p < 0.05$, $p = 0.09$, $p < 0.01$ respectively), together with
513 increased SOCS3 (Figure supplement 7I, 7J; $p < 0.01$, $p < 0.05$ respectively). Validation of
514 a pharmacological hyperleptinemia model allowed us to access ovarian samples from
515 mice with hyperactivation of ObRb, here indicated by increased SOCS3 expression, but
516 lacking the remaining traits of obesity.

517 Next, we collected CCs from superovulated mice after LEPT treatment and
518 analysed their transcriptome (Figure 4A). After DESeq2 analysis (FDR < 0.05), a total
519 of 2026 differently expressed genes were found between LEPT and CONT samples

520 (1212 genes upregulated and 814 downregulated) (Figure 4B). Gene ontology analysis
521 of the DEG lists showed that the upregulated genes for LEPT were associated primarily
522 with cellular organisation, the cytoskeleton and immune responses, supporting the
523 immune-mediating role of leptin as evidenced before (40–42). Conversely, amongst the
524 LEPT downregulated pathways were cell metabolism as well as chromatin organisation
525 and histone modifications (Figure supplement 8; Table 9). Next, based on the
526 hypothesis that early-onset obesity is followed by hyperactivation of leptin signalling in
527 the ovary, we overlapped both 4wk DIO model and LEPT transcriptome datasets,
528 aiming to pinpoint the LEPT driven effects in the CC transcriptome during early obesity.
529 PCA revealed the clustering of 4 wk DIO and CONT samples, and LEPT samples apart
530 (Figure 4C). Indeed, leptin treatment seemed to drive PC1. Next, we overlapped the
531 DEGs from 4 wk HFD and LEPT protocols and found 144 genes upregulated in both
532 LEPT and 4 wk HFD. These were related to response to toxins, transport and glucose
533 metabolism (Figure 4D; Table 10). More specifically, the genes *Lipocalin (Lcn) 2*,
534 *Anxa11* and *Glucose-6-phosphate dehydrogenase x-linked (G6pdx)* were amongst the
535 most significant (Figure 4D). Conversely, the GO terms associated with the 177
536 downregulated genes in both protocols were metabolism and gene expression regulation
537 (Figure 4D; Table 10). A number of downregulated genes were found to encode
538 important epigenetic factors, such as *Dna segment, chr 14, abbott 1 expressed o (Tasor)*,
539 *Lysine (k)-specific methyltransferase 2d (Kmt2d/Mll2)*, *Methyl-cpg binding domain*
540 *protein (Mbd) 2*, and *DNA methyltransferase (Dnmt) 3a* (Figure 4E), which suggested
541 epigenetic dysregulation. Another important effect that could be attributed to leptin in
542 early stages of obesity was the repression of genes mediating actin-cytoskeleton
543 reorganisation (Figure 4F; Table 9). Furthermore, we assessed the potential impact of
544 leptin on genes involved in CC metabolism, and verified the role of leptin on glucose
545 metabolism (Figure 4G) and fatty acid oxidation (Figure 4H), which was reflected in the
546 similarities between LEPT and 4 wk HFD. Here, we questioned how lack of leptin
547 signalling could be detrimental metabolically. For instance, the oocyte is unable to
548 metabolise glucose due to low phosphofructokinase activity (43), highlighting the
549 importance of glycolytic activity of CCs in the generation of pyruvate (44). This
550 function appeared to be decreased in 16 wk HFD, which could be the result of the
551 establishment of leptin resistance in the ovary. As a consequence, the transport of
552 pyruvate into the oocyte would be decreased, which could directly impact the
553 tricarboxylic acid cycle (TCA) and adenosine triphosphate (ATP) generation (Figure
554 supplement 9B) (45). Leptin is also known to be key for free fatty acid (FFA)

555 metabolism, promoting their oxidation and regulating the homeostasis of triglycerides in
556 a cell (46,47). Thus, disruption of leptin signalling in 16 wk HFD CCs (Figure
557 supplement 9A) could be relevant for lipotoxicity and stress previously described in
558 obese ovaries (48) (Figure supplement 9E, 9F). In general, hyperactivation of leptin
559 signalling in CCs seemed to be linked primarily to impaired cell membrane transport
560 and endocytosis, but also cell metabolism and gene expression regulation.

561

562 **DISCUSSION**

563 The present study characterises the molecular mechanisms underlying the establishment
564 of leptin resistance in the ovary of DIO mice. Furthermore, making use of sensitive
565 methods for reduced-cell number RNA-seq, we studied the transcriptome of the somatic
566 cells surrounding the oocyte from mice subjected to DIO for 4 wk and 16 wk, as well as
567 validated model for pharmacological hyperleptinemia – a system presenting exclusively
568 increased circulating levels of leptin amongst all features of obesity, which allowed us
569 to pinpoint the exclusive effects of leptin-SOCS3 ovarian hyperactivation during early-
570 onset of obesity.

571 Leptin is a major adipokine, which was initially linked to satiety (6). The
572 establishment of leptin resistance at different levels in the body has been documented in
573 recent years as one of the outcomes of obesity. Accordingly, leptin signalling is
574 deregulated in the hypothalamus (49) and liver of obese human and mice (50). However,
575 the same was not found in kidney (51) or heart (52) of obese humans, suggesting an
576 organ-specific response. We confirmed here, for the first time, the establishment of
577 leptin resistance in the ovary of obese female mice. This poses very important questions
578 on the long-term effects of obesity on ovarian performance, concerning the known local
579 roles of leptin on follicular growth (12), ovulation (13), and oocyte quality (53). Leptin
580 action in the ovary is highly intricate and its effects bimodal. Low leptin levels in
581 circulation facilitate the transition from primary to secondary follicles (12), but leptin is
582 also required for ovulation, possibly supporting CC expansion through cyclooxygenase
583 (COX) 2 and hyaluronic acid synthase (HAS) 2 activity (13). Indeed, *ob/ob* mice
584 contain antral follicles in their ovaries (data not shown), but fail to ovulate. Thus, during
585 obesity progression, altered leptin signalling in the ovary could lead to functional failure
586 and infertility through different mechanisms, mainly characterised by the
587 hyperactivation of ObRb in the onset of obesity and complete failure in signalling in
588 late obesity.

589 Our first aim was to elucidate the molecular mechanisms leading to the
590 establishment of leptin resistance in the obese ovary. The analysis of different ObRb
591 Tyr domains highlighted the decrease in pTyr985 along with pJAK2 in ovaries from 16
592 wk HFD mice, concomitant with the increase in SOCS3 protein and decrease in
593 pSTAT5. Functionally, STAT5 phosphorylation in the mouse ovary was shown to be
594 crucial for prolactin signalling and cell proliferation during follicular growth (54), as
595 well as corpus luteum formation (55). Hence, reduced pSTAT5 signalling *per se* could
596 compromise oocyte maturation and fertility during obesity. Importantly, we observed
597 that SOCS3 staining in the oocyte occurred mainly in response to ObRb activation,
598 since the *ob/ob* mouse presented weaker staining. This suggests a direct impact of
599 disrupted ovarian leptin signalling on oocyte quality through SOCS3 activation. Indeed,
600 at 16 wk DIO, we observed different levels of *Socs3* transcribed in various ovarian
601 components. Our RNA-seq data revealed that *Socs3* was increased at 4 wk HFD, but
602 decreased at 16 wk HFD in CCs, whereas in the TC fraction it was upregulated at both
603 time points. This may suggest blunted ObRb signalling in CCs at 16 wks HFD, once the
604 transcription of the major components of the pathway was inhibited (Figure supplement
605 9A). Therefore, leptin signalling in CCs seems to be highly sensitive to obesity and
606 maternal metabolic performance.

607 Having an understanding of the impact of obesity on leptin signalling in the
608 ovary, we then analysed the transcriptome of CCs from DIO mice. A major observation
609 of this study was the striking correlation between BW and the global gene expression
610 profile of CCs. On the other hand, other studies showed functional changes in the ovary,
611 including depletion of primordial follicles and inflammation in HFD mice, irrespective
612 of gain in BW (56). Differences in diet composition, as well as variable length of
613 exposure to diet, might account for the differences between studies. Also the
614 aforementioned study did not present a global gene expression analysis. Interestingly,
615 when found that the expression profile of HFD-DEGs in the HFDLG CCs was similar
616 to that in 16 wk CD, clearly demonstrating the impact of maternal BW, which probably
617 largely reflects adiposity in this model, on gene expression in CCs.

618 Another major outcome of the transcriptome analysis of CCs was the
619 identification of gene signatures altered in early vs late stages of obesity. After 4 wk
620 HFD, mainly genes involved in glucose metabolism and cell membrane trafficking were
621 differently expressed. The use of the pharmacologically hyperleptinemic model allowed
622 us to dissect the contribution of hyperactivation of ObRb to the major changes taking
623 place in CCs in early obesity. Increased activation of the JAK-STAT cascade seemed

624 mainly to impair cellular trafficking and paracrine transfer of macromolecules. This is
625 known to be a crucial process for the metabolic cooperation between the oocyte and
626 somatic cells (23). Cell trafficking and nutrient mobilisation to the oocyte, as well as the
627 uptake of signalling molecules from the oocyte, is fundamental for COCs expansion and
628 oocyte maturation (23). Indeed, the genes *Micall1* and *Unc-51 Like Kinase (Ulk) 4* are
629 important mediators of endocytosis, and were shown to be regulated by *Stat3* (57,58).
630 Furthermore, amongst the genes upregulated in both 4wk HFD and LEPT we found
631 *Lcn2*, associated with lipid and hormone transport (59), *Claudine (Cldn) 22*, a
632 component of tight junctions (60), and *Anxa11*, known to be involved in transmembrane
633 secretion (61). This is suggestive of the effects of leptin in altering transmembrane
634 transport in the early-onset of obesity.

635 We also identified the metabolic gene *Arachidonate 15-Lipoxygenase (Alox15)*,
636 and the transcription factor *Hes Related Family BHLH Transcription Factor With*
637 *YRPW Motif (Hey) 1*, were amongst the most significantly upregulated genes in both 4
638 wk HFD and LEPT (Table 10). The transcriptional repressor HEY1 is directly activated
639 by Notch Receptor (NOTCH) 2 during follicular development, and both HEY1 and
640 NOTCH2 were shown to be increased in proliferating granulosa cells and can contribute
641 to ovarian overstimulation and premature follicular failure (62). These effects further
642 demonstrate the detrimental role of increased ObRb activation during the onset of
643 obesity in cell trafficking and immune response.

644 Amongst the downregulated signatures in both 4 wk HFD and LEPT we found
645 genes that encoded for important epigenetic factors, such as *Tasor*, *Kmt2d/Mll2*, *Mbd2*,
646 and *Dnmt3a* (Figure 4D, table 10), which could indicate epigenetic dysregulation in
647 these cells in early obesity being mediated by leptin. Another striking result was the
648 coordinate downregulation of genes involved in cytoskeleton and actin-filament
649 organisation again in 4 wk HFD and LEPT. As in axons, microtubules form the
650 cytoskeletal core of granulosa cell transzonal projections (TZPs), which provide tracks
651 for the polarized translocation of secretory pathway organelles (63). Thus, by impairing
652 the intrinsic stability of TZPs in granulosa cells, leptin could be affecting the paracrine
653 exchanges between oocytes and somatic cells, an instrumental system for oocyte
654 maturation (64). Indeed, the oocyte is in extreme need of the metabolites generated in
655 CCs, but also signalling factors such as growth differentiation factor (GDF) 9 secreted
656 by the oocyte and required to orchestrate CCs function. Leptin seemed to support the
657 TCA cycle at 4 wk HFD (Figure supplement 9B), which suggested to us that at this
658 early stage the boost in leptin signalling in CCs could actually have beneficial effects,

659 following the positive response on oocyte competence and GDF9 signalling (Figure
660 supplement 9D). However, at 16 wk HFD the inferred drop in CC metabolic fitness was
661 paralleled by a decrease in the main paracrine mediators of oocyte maturation and
662 responsiveness to GDF9 (Figure supplement 9B-D), which invariably suggest
663 compromised oocyte quality. The aforementioned events are an important part of COC
664 expansion, a complex mechanism triggered by luteinizing hormone (LH), in which
665 bidirectional exchange of metabolites and signalling factors between the oocyte and
666 CCs leads to maturation of the gamete and resumption of meiosis (22). This process is
667 tightly regulated by immune mediators, particularly interleukin (IL) 6 (65). Indeed, as
668 well as being highlighted in our transcriptome analysis, the role of leptin in the
669 inflammatory response, in particular mediating innate immunity through IL6, has been
670 described before (55). Consequently, the detrimental effect of obesity could be related
671 to increased leptin signalling at 4 wk HFD, but most likely through its failure at 16 wk
672 HFD (Figure supplement 9A). Generally, in the early stages of obesity, leptin
673 downregulated potentially important epigenetic mediators and genes involved in
674 cytoskeletal organisation in CCs.

675 The analysis of 16 wk HFD DEGs, as well as the profile of temporal changes
676 revealed genes involved in cell trafficking as *Micall1* or *Dync1h*, involved in protein
677 transport, positioning of cell compartments, and movement of structures within the cell
678 (66) to be decreased in 4 wk and 16 wk HFD. Furthermore, the most increased gene in
679 16 wk HFD was the *Guanylate-binding protein (Gbp) 8* (Table 7), a component of
680 cellular response to interferon-gamma (67). Another gene upregulated at 16 wk HFD
681 was *Rhou*, a gene that regulates cell morphology (68). Considering also the high
682 expression level of inflammatory mediators at this stage, the activated pathways may
683 well be an outcome of lipotoxicity previously described in the obese ovary (48). Thus,
684 during obesity ovarian cells are trying to accommodate the surplus of lipid compounds,
685 which is likely to activate mechanisms of cellular reorganisation. Overall, early changes
686 in CC transport, gene expression and epigenetic regulation are followed by mounting
687 inflammatory pathways and cellular rearrangement to accommodate the lipid surplus.

688 In conclusion, we found that the ovaries of obese mice develop leptin resistance
689 and that global gene expression in CCs was strikingly correlated with BW.
690 Mechanistically, failure in ovarian leptin signalling was mediated by SOCS3
691 overexpression, and inhibition of pTyr985 and pJAK2. Initially, during the onset of
692 obesity the hyperactivation of leptin signalling was linked to increased expression of
693 genes for cell trafficking and cytoskeleton organisation, and inhibition of genes

694 associated with epigenetic regulations in CCs. Conversely, in late obesity, altered gene
695 signatures were mainly linked to inflammatory response and morphological
696 rearrangement (Figure 5). This analysis revealed for the first time the temporal changes
697 in gene expression in CCs during obesity progression. Further studies are being
698 undertaken to understand the impact of these changes in oocyte and early embryo
699 development.

700

701 **ACKNOWLEDGEMENTS**

702 We would like to thank Dr Leslie Paul Kozak and Dr Magdalena Jura for their support
703 with the validation and characterisation of the mouse obese phenotype; Dr Jorg Morf for
704 the constructive discussion and suggestions on the analysis of the transcriptome data; Dr
705 Daniel Murta for providing the of mouse ovarian slides; and Dr Fatima Santos and Dr
706 Krzysztof Witek for their support with the imaging and confocal microscopy.

707

708 **STATEMENT OF ETHICS**

709 Animal experiments conform to internationally accepted standards and have been
710 approved by the appropriate institutional review body.

711

712 **DISCLOSURE STATEMENT**

713 The authors have no conflict of interest to declare.

714

715 **FOUNDING SOURCES**

716 Work was supported by grants from the Polish National Centre for Science (No.
717 2014/15/D/NZ4/01152 and 2016/23/B/NZ4/03737) awarded to A. G. and the UK
718 Biotechnology and Biological Sciences Research Council and Medical Research
719 Council (BBS/E/B/000C0423, MR/K011332/1, MR/S000437/1) awarded to G.K.; A. G.
720 was supported by Horizon 2020 Marie Curie Individual Fellowship; Processing charge
721 covered by the KNOW Consortium: “Healthy Animal - Safe Food” (Ministry of
722 Sciences and Higher Education; Dec: 05-1/KNOW2/2015).

723

724 **AUTHORS CONTRIBUTION**

725 KW data acquisition, analysis and interpretation of the data, writing the manuscript; EW
726 data acquisition, analysis and interpretation of the data; MA, data acquisition and
727 analysis; JCF bioinformatic analysis and interpretation of data, revising the manuscript;
728 GK supervision, funding, revising the manuscript; AG conception and design, funding

729 acquisition, acquisition of data, bioinformatic analysis and interpretation of data, writing
730 and revising of the manuscript.

731

732 REFERENCES

733

- 734 1. Schelbert KB. Comorbidities of Obesity. *Prim Care Clin Off Pract*. 2009 Jun
735 1;36(2):271–85.
- 736 2. Pasquali R, Patton L, Gambineri A. Obesity and infertility. *Curr Opin Endocrinol*
737 *Diabetes Obes*. 2007 Dec;14(6):482–7.
- 738 3. Dağ ZÖ, Dilbaz B. Impact of obesity on infertility in women. *J Turkish Ger*
739 *Gynecol Assoc*. 2015;16(2):111–7.
- 740 4. Unger RH, Zhou YT. Lipotoxicity of beta-cells in obesity and in other causes of
741 fatty acid spillover. *Diabetes*. 2001 Feb 1;50 Suppl 1(suppl 1):S118-21.
- 742 5. Robker RL, Wu LL-Y, Yang X. Inflammatory pathways linking obesity and
743 ovarian dysfunction. *J Reprod Immunol*. 2011 Mar;88(2):142–8.
- 744 6. Friedman JM, Halaas JL. Leptin and the regulation of body weight in mammals.
745 *Nature*. 1998 Oct 22;395(6704):763–70.
- 746 7. Maffei M, Halaas J, Ravussin E, Pratley RE, Lee GH, Zhang Y, et al. Leptin
747 levels in human and rodent: Measurement of plasma leptin and ob RNA in obese
748 and weight-reduced subjects. *Nat Med*. 1995;1(11):1155–61.
- 749 8. Vaisse C, Halaas JL, Horvath CM, Darnell JE, Stoffel M, Friedman JM. Leptin
750 activation of Stat3 in the hypothalamus of wild-type and ob/ob mice but not
751 db/db mice. *Nat Genet*. 1996 Sep 1;14(1):95–7.
- 752 9. Cava A La, Matarese G. The weight of leptin in immunity. *Nat Rev Immunol*.
753 2004 May 1;4(5):371–9.
- 754 10. Sierra-Honigmann MR, Nath AK, Murakami C, Garcia-Cardena G,
755 Papapetropoulos A, Sessa WC, et al. Biological action of leptin as an angiogenic
756 factor 1. *Science (80-)*. 1998;281(0036-8075 (Print)):1683–6.
- 757 11. Quennell JH, Mulligan AC, Tups A, Liu X, Phipps SJ, Kemp CJ, et al. Leptin
758 Indirectly Regulates Gonadotropin-Releasing Hormone Neuronal Function.
759 *Endocrinology*. 2009 Jun;150(6):2805–12.
- 760 12. Panwar S, Herrid M, Kauter KG, McFarlane JR. Effect of passive immunization
761 against leptin on ovarian follicular development in prepubertal mice. *J Reprod*
762 *Immunol*. 2012 Dec 1;96(1–2):19–24.
- 763 13. Dupuis L, Schuermann Y, Cohen T, Siddappa D, Kalaiselvanraja A, Pansera M,

- 764 et al. Role of leptin receptors in granulosa cells during ovulation. *Reproduction*.
765 2013 Dec 19;147(2):221–9.
- 766 14. Herrid M, Nguyen VL, Hinch G, McFarlane JR. Leptin has concentration and
767 stage-dependent effects on embryonic development in vitro. *Reproduction*. 2006
768 Aug 1;132(2):247–56.
- 769 15. Ryan NK, Woodhouse CM, Van der Hoek KH, Gilchrist RB, Armstrong DT,
770 Norman RJ. Expression of Leptin and Its Receptor in the Murine Ovary: Possible
771 Role in the Regulation of Oocyte Maturation1. *Biol Reprod*. 2002 May
772 1;66(5):1548–54.
- 773 16. Kloek C, Haq AK, Dunn SL, Lavery HJ, Banks AS, Myers MG. Regulation of
774 Jak kinases by intracellular leptin receptor sequences. *J Biol Chem*. 2002 Nov
775 1;277(44):41547–55.
- 776 17. Banks AS, Davis SM, Bates SH, Myers MG. Activation of downstream signals
777 by the long form of the leptin receptor. *J Biol Chem*. 2000 May
778 12;275(19):14563–72.
- 779 18. Mütze J, Roth J, Gerstberger R, Hübschle T. Nuclear translocation of the
780 transcription factor STAT5 in the rat brain after systemic leptin administration.
781 *Neurosci Lett*. 2007 May 7;417(3):286–91.
- 782 19. Bjørnbæk C, Lavery HJ, Bates SH, Olson RK, Davis SM, Flier JS, et al. SOCS3
783 Mediates Feedback Inhibition of the Leptin Receptor via Tyr⁹⁸⁵. *J Biol Chem*.
784 2000 Dec 22;275(51):40649–57.
- 785 20. Zabolotny JM, Bence-Hanulec KK, Stricker-Krongrad A, Haj F, Wang Y,
786 Minokoshi Y, et al. PTP1B regulates leptin signal transduction in vivo. *Dev Cell*.
787 2002 Apr;2(4):489–95.
- 788 21. Sugiura K, Pendola FL, Eppig JJ. Oocyte control of metabolic cooperativity
789 between oocytes and companion granulosa cells: energy metabolism. *Dev Biol*.
790 2005 Mar 1;279(1):20–30.
- 791 22. Dumesic DA, Meldrum DR, Katz-Jaffe MG, Krisher RL, Schoolcraft WB.
792 Oocyte environment: follicular fluid and cumulus cells are critical for oocyte
793 health. *Fertil Steril*. 2015 Feb;103(2):303–16.
- 794 23. Russell DL, Gilchrist RB, Brown HM, Thompson JG. Bidirectional
795 communication between cumulus cells and the oocyte: Old hands and new
796 players? *Theriogenology*. 2016 Jul 1;86(1):62–8.
- 797 24. Vigone G, Merico V, Prigione A, Mulas F, Sacchi L, Gabetta M, et al.
798 Transcriptome based identification of mouse cumulus cell markers that predict

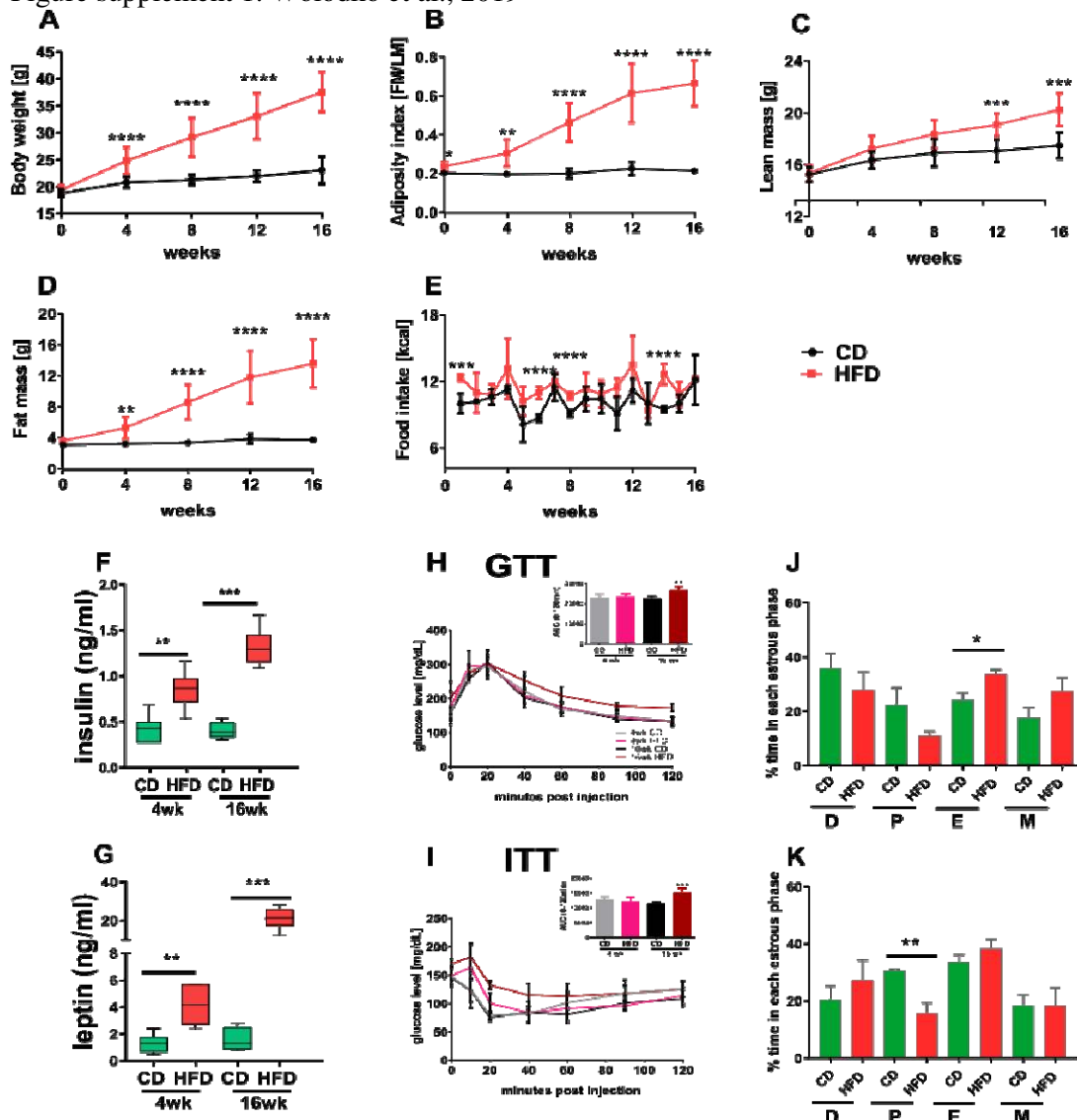
- 799 the developmental competence of their enclosed antral oocytes. *BMC Genomics*.
800 2013;14(1):380.
- 801 25. Uyar A, Torrealday S, Seli E. Cumulus and granulosa cell markers of oocyte and
802 embryo quality. In: *Fertility and Sterility*. 2013. p. 979–97.
- 803 26. Kyrönlahti A, Vetter M, Euler R, Bielinska M, Jay PY, Anttonen M, et al.
804 GATA4 Deficiency Impairs Ovarian Function in Adult Mice¹. *Biol Reprod*.
805 2011 May 1;84(5):1033–44.
- 806 27. Couse JF, Yates MM, Rodriguez KF, Johnson JA, Poirier D, Korach KS. The
807 Intraovarian Actions of Estrogen Receptor- α Are Necessary to Repress the
808 Formation of Morphological and Functional Leydig-Like Cells in the Female
809 Gonad. *Endocrinology*. 2006 Aug;147(8):3666–78.
- 810 28. Koressaar T, Remm M. Enhancements and modifications of primer design
811 program Primer3. *Bioinformatics*. 2007 May 15;23(10):1289–91.
- 812 29. Galvão A, Wolodko K, Rebordão MR, Skarzynski D, Ferreira-Dias G. TGFB1
813 modulates in vitro secretory activity and viability of equine luteal cells. *Cytokine*.
814 2018 Oct 1;110:316–27.
- 815 30. Zhao S, Fernald RD. Comprehensive Algorithm for Quantitative Real-Time
816 Polymerase Chain Reaction. *J Comput Biol*. 2005 Oct 21;12(8):1047–64.
- 817 31. Picelli S, Björklund ÅK, Faridani OR, Sagasser S, Winberg G, Sandberg R.
818 Smart-seq2 for sensitive full-length transcriptome profiling in single cells. *Nat*
819 *Methods*. 2013 Nov 22;10(11):1096–8.
- 820 32. Picelli S, Faridani OR, Björklund ÅK, Winberg G, Sagasser S, Sandberg R. Full-
821 length RNA-seq from single cells using Smart-seq2. *Nat Protoc*. 2014 Jan
822 2;9(1):171–81.
- 823 33. Love MI, Huber W, Anders S. Moderated estimation of fold change and
824 dispersion for RNA-seq data with DESeq2. *Genome Biol*. 2014 Dec
825 5;15(12):550.
- 826 34. Duan J, Choi Y-H, Hartzell D, Della-Fera MA, Hamrick M, Baile CA. Effects of
827 Subcutaneous Leptin Injections on Hypo-thalamic Gene Profiles in Lean and
828 ob/ob Mice. 2007.
- 829 35. Eden E, Lipson D, Yogev S, Yakhini Z. Discovering Motifs in Ranked Lists of
830 DNA Sequences. *PLoS Comput Biol*. 2007 Mar 23;3(3):e39.
- 831 36. Eden E, Navon R, Steinfeld I, Lipson D, Yakhini Z. GOrilla: a tool for discovery
832 and visualization of enriched GO terms in ranked gene lists. *BMC Bioinformatics*.
833 2009 Dec 3;10(1):48.

- 834 37. Assou S, Haouzi D, Mahmoud K, Aouacheria A, Guillemin Y, Pantesco V, et al.
835 A non-invasive test for assessing embryo potential by gene expression profiles of
836 human cumulus cells: a proof of concept study. *Mol Hum Reprod*. 2008 Dec
837 1;14(12):711–9.
- 838 38. Gebhardt KM, Feil DK, Dunning KR, Lane M, Russell DL. Human cumulus cell
839 gene expression as a biomarker of pregnancy outcome after single embryo
840 transfer. *Fertil Steril*. 2011;96(1).
- 841 39. Assou S, Haouzi D, De Vos J, Hamamah S. Human cumulus cells as biomarkers
842 for embryo and pregnancy outcomes. *Mol Hum Reprod*. 2010 Aug 1;16(8):531–8.
- 843 40. Iikuni N, Lam QLK, Lu L, Matarese G, La Cava A. Leptin and Inflammation.
844 *Curr Immunol Rev*. 2008 May 1;4(2):70–9.
- 845 41. Faggioni R, Fantuzzi G, Fuller J, Dinarello CA, Feingold KR, Grunfeld C. IL-1 β
846 mediates leptin induction during inflammation. *Am J Physiol Integr Comp*
847 *Physiol*. 1998 Jan;274(1):R204–8.
- 848 42. Fantuzzi G, Faggioni R. Leptin in the regulation of immunity, inflammation, and
849 hematopoiesis. *J Leukoc Biol*. 2000 Oct;68(4):437–46.
- 850 43. Cetica P, Pintos L, Dalvit G, Beconi M. Activity of key enzymes involved in
851 glucose and triglyceride catabolism during bovine oocyte maturation in vitro.
852 *Reproduction*. 2002 Nov;124(5):675–81.
- 853 44. Thompson JG, Lane M, Gilchrist RB. Metabolism of the bovine cumulus-oocyte
854 complex and influence on subsequent developmental competence. *Soc Reprod*
855 *Fertil Suppl*. 2007;64:179–90.
- 856 45. Sutton-McDowall ML, Gilchrist RB, Thompson JG. The pivotal role of glucose
857 metabolism in determining oocyte developmental competence.
858 *REPRODUCTION*. 2010 Apr;139(4):685–95.
- 859 46. Yamagishi S, Edelstein D, Du X, Kaneda Y, Guzmán M, Brownlee M. Leptin
860 Induces Mitochondrial Superoxide Production and Monocyte Chemoattractant
861 Protein-1 Expression in Aortic Endothelial Cells by Increasing Fatty Acid
862 Oxidation via Protein Kinase A. *J Biol Chem*. 2001 Jul 6;276(27):25096–100.
- 863 47. Unger RH, Zhou YT, Orci L. Regulation of fatty acid homeostasis in cells: novel
864 role of leptin. *Proc Natl Acad Sci U S A*. 1999 Mar 2;96(5):2327–32.
- 865 48. Wu LL-Y, Dunning KR, Yang X, Russell DL, Lane M, Norman RJ, et al. High-
866 Fat Diet Causes Lipotoxicity Responses in Cumulus–Oocyte Complexes and
867 Decreased Fertilization Rates. *Endocrinology*. 2010 Nov;151(11):5438–45.
- 868 49. Münzberg H, Flier JS, Bjørnbæk C. Region-Specific Leptin Resistance within the

- 869 Hypothalamus of Diet-Induced Obese Mice. *Endocrinology*. 2004 Nov
870 1;145(11):4880–9.
- 871 50. Brabant G, Müller G, Horn R, Anderwald C, Roden M, Nave H. Hepatic leptin
872 signaling in obesity. *FASEB J*. 2005;19(8):1048–50.
- 873 51. Morgan DA, Thedens DR, Weiss R, Rahmouni K. Mechanisms mediating renal
874 sympathetic activation to leptin in obesity. *Am J Physiol Integr Comp Physiol*.
875 2008 Dec;295(6):R1730–6.
- 876 52. Mark AL, Correia MLG, Rahmouni K, Haynes WG. Selective leptin resistance: a
877 new concept in leptin physiology with cardiovascular implications. *J Hypertens*.
878 2002 Jul;20(7):1245–50.
- 879 53. Joo J-K, Joo B-S, Kim S-C, Choi J-R, Park S-H, Lee K-S. Role of leptin in
880 improvement of oocyte quality by regulation of ovarian angiogenesis. *Anim*
881 *Reprod Sci*. 2010 Jun;119(3–4):329–34.
- 882 54. Bouilly J, Sonigo C, Auffret J, Gibori G. Prolactin signaling mechanisms in
883 ovary. *Mol Cell Endocrinol*. 2012 Jun 5;356(1–2):80–7.
- 884 55. Fernández-Riejos P, Najib S, Santos-Alvarez J, Martín-Romero C, Pérez-Pérez A,
885 González-Yanes C, et al. Role of Leptin in the Activation of Immune Cells.
886 *Mediators Inflamm*. 2010;2010:1–8.
- 887 56. Skaznik-Wikiel ME, Swindle DC, Allshouse AA, Polotsky AJ, McManaman JL.
888 High-Fat Diet Causes Subfertility and Compromised Ovarian Function
889 Independent of Obesity in Mice¹. *Biol Reprod*. 2016 May 1;94(5).
- 890 57. Pelkmans L, Fava E, Grabner H, Hannus M, Habermann B, Krausz E, et al.
891 Genome-wide analysis of human kinases in clathrin- and caveolae/raft-mediated
892 endocytosis. *Nature*. 2005 Jul 11;436(7047):78–86.
- 893 58. Giridharan SSP, Cai B, Vitale N, Naslavsky N, Caplan S. Cooperation of
894 MICAL-L1, syndapin2, and phosphatidic acid in tubular recycling endosome
895 biogenesis. Lemmon S, editor. *Mol Biol Cell*. 2013 Jun;24(11):1776–90.
- 896 59. Wang Y. Small lipid-binding proteins in regulating endothelial and vascular
897 functions: focusing on adipocyte fatty acid binding protein and lipocalin-2. *Br J*
898 *Pharmacol*. 2012 Feb;165(3):603–21.
- 899 60. Günzel D, Yu ASL. Claudins and the modulation of tight junction permeability.
900 *Physiol Rev*. 2013;93(2):525–69.
- 901 61. Mirsaeidi M, Gidfar S, Vu A, Schraufnagel D. Annexins family: insights into
902 their functions and potential role in pathogenesis of sarcoidosis. *J Transl Med*.
903 2016 Dec 12;14(1):89.

- 904 62. Vanorny DA, Mayo KE. The role of Notch signaling in the mammalian ovary.
905 Reproduction. 2017 Jun;153(6):R187–204.
- 906 63. Albertini DF, Combelles CM, Benecchi E, Carabatsos MJ. Cellular basis for
907 paracrine regulation of ovarian follicle development. *Reproduction*. 2001
908 May;121(5):647–53.
- 909 64. Li R, Albertini DF. The road to maturation: somatic cell interaction and self-
910 organization of the mammalian oocyte. *Nat Rev Mol Cell Biol*. 2013 Mar
911 22;14(3):141–52.
- 912 65. Liu Z, de Matos DG, Fan H-Y, Shimada M, Palmer S, Richards JS. Interleukin-6:
913 An Autocrine Regulator of the Mouse Cumulus Cell-Oocyte Complex Expansion
914 Process. *Endocrinology*. 2009 Jul;150(7):3360–8.
- 915 66. Vaisberg EA, Grissom PM, McIntosh JR. Mammalian cells express three distinct
916 dynein heavy chains that are localized to different cytoplasmic organelles. *J Cell*
917 *Biol*. 1996 May 1;133(4):831–42.
- 918 67. Tripal P, Bauer M, Naschberger E, Mörtinger T, Hohenadl C, Cornali E, et al.
919 Unique Features of Different Members of the Human Guanylate-Binding Protein
920 Family. *J Interf Cytokine Res*. 2007 Jan 31;27(1):44–52.
- 921 68. Tao W, Pennica D, Xu L, Kalejta RF, Levine AJ. Wrch-1, a novel member of the
922 Rho gene family that is regulated by Wnt-1. *Genes Dev*. 2001 Jul
923 15;15(14):1796–807.
- 924 69. Bilbao MG, Di Yorio MP, Faletti AG. Different levels of leptin regulate different
925 target enzymes involved in progesterone synthesis. *Fertil Steril*. 2013
926 Apr;99(5):1460–6.
- 927 70. Di Yorio MP, Bilbao MG, Pustovrh MC, Prestifilippo JP, Faletti AG. Leptin
928 modulates the expression of its receptors in the hypothalamic-pituitary-ovarian
929 axis in a differential way. *J Endocrinol*. 2008 Aug 1;198(2):355–66.
- 930 71. Yang W-H, Liu S-C, Tsai C-H, Fong Y-C, Wang S-J, Chang Y-S, et al. Leptin
931 Induces IL-6 Expression through OBRI Receptor Signaling Pathway in Human
932 Synovial Fibroblasts. Sanchez-Margalet V, editor. *PLoS One*. 2013 Sep
933 27;8(9):e75551.
- 934 72. Loffreda S, Yang SQ, Lin HZ, Karp CL, Brengman ML, Wang DJ, et al. Leptin
935 regulates proinflammatory immune responses. *FASEB J*. 1998;12(1):57–65.
- 936

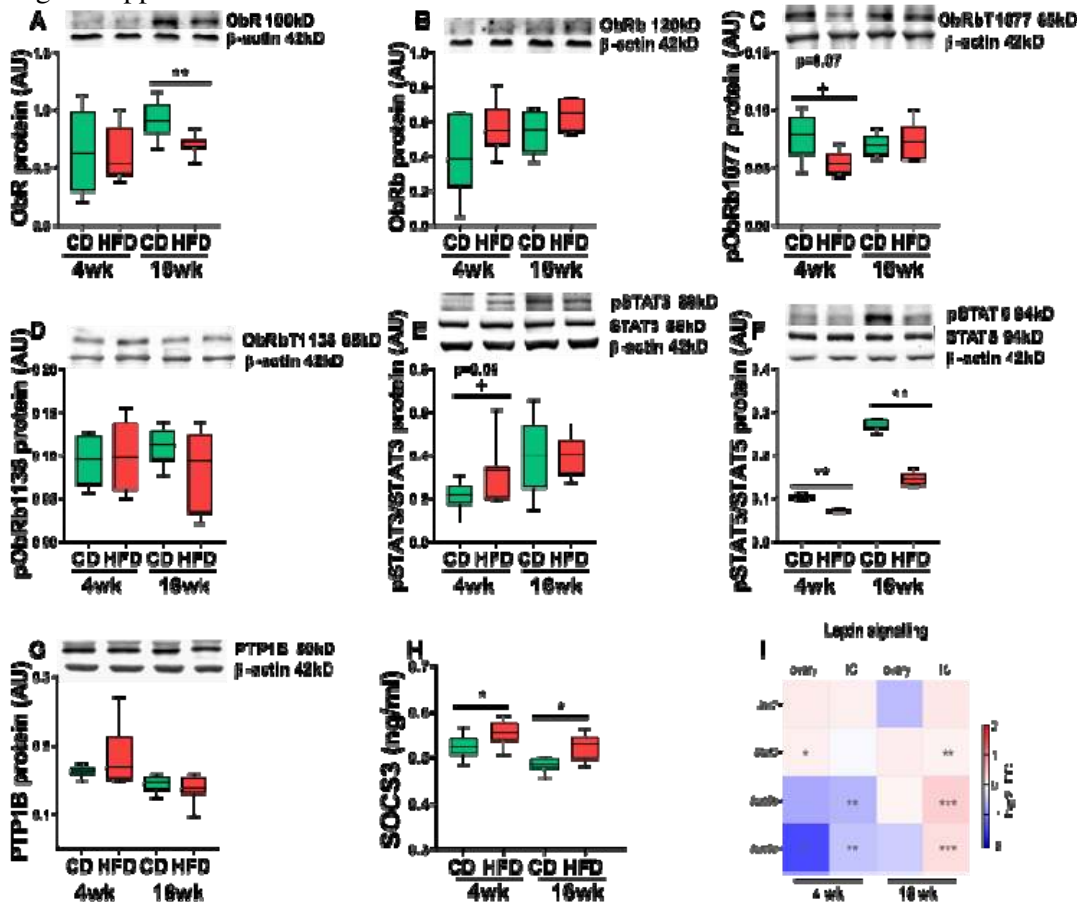
1 Figure supplement 1. Wołodko et al., 2019



2
3 **Figure supplement 1. Phenotype characterisation of diet-induced obese mice.**
4 Changes in (A) body weight, (B) adiposity index, (C) lean mass, (D) fat mass, (E) food
5 intake in mice fed chow diet (CD, black line) and high fat diet (HFD, red line) for 4 or
6 16 weeks (wk). Plasma level of (F) insulin and (G) leptin in mice fed CD or HFD for 4
7 and 16 wk. Glucose tolerance test (GTT, H) and insulin tolerance test (ITT, I) present
8 glucose levels at 0-120 min after glucose and insulin injection, respectively. Bar graphs
9 in the upper right panel present area under the curve for each group. Plasma collected
10 from animals in oestrus phase. Proportion of time spent in each oestrous phase of mice
11 subjected to CD or HFD for 4 wk (J) and 16 wk (K) monitored for 12 days. D,
12 dioestrus; E, oestrus; M, metoestrus; P, pro-oestrus. Each bar represents the mean \pm SD
13 for $n=12$. Differences in phenotype characteristics and plasma hormone level between
14 groups were analysed by Mann-Whitney test, oestrous cycle distribution analysed by
15 unpaired t-test. * $p<0.05$; ** $p<0.01$; *** $p<0.001$.

16
17
18

19 Figure supplement 2. Wołodko et al. 2019



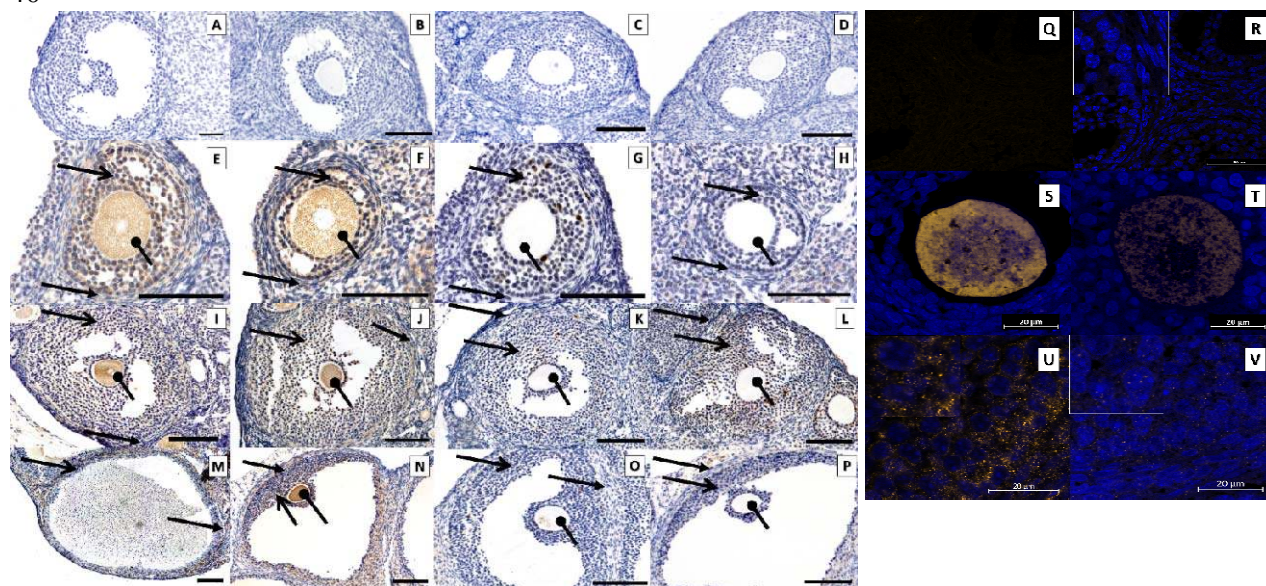
20
21
22
23
24
25
26
27
28
29
30
31
32
33
34
35
36
37
38

Figure supplement 2. Expression of leptin signalling components in the ovary of diet induced obese mice.

Protein abundance of components of the leptin signalling pathway in ovarian extracts analysed by Western blot or ELISA. Animals were maintained on chow diet (CD) or high fat diet (HFD) for 4 or 16 weeks (wk). Abundance of (A) leptin receptor (ObR), phosphorylation of (B) long isoform of leptin receptor (ObRb), (C) tyrosine 1077 of leptin receptor, (D) tyrosine 1138 of leptin receptor, (E) STAT3, (F) STAT5, expression of (G) PTP1B. (H) SOCS3 ovarian quantification in ELISA test. (I) Heatmap showing fold of change in expression of mRNA of leptin signalling components measured in whole ovary or theca/stroma enriched (TC) fraction by RT-PCR. mRNA expression of *Rpl37* and protein expression of β -actin were used to normalize the expression data. Each bar represents the mean \pm SD. Differences between groups were analysed by Mann-Whitney test. N=4-8 for immunoblots and N=8 for RT-PCR analysis and ELISA. * $p < 0.05$; ** $p < 0.01$; *** $p < 0.001$; + $p = 0.06$ or $p = 0.07$.

39 Figure supplement 3. Wołodko et al., 2019

40



44

45 **Figure supplement 3. Immunolocalisation of SOCS3 and PTP1B protein in the**
46 **ovary.**

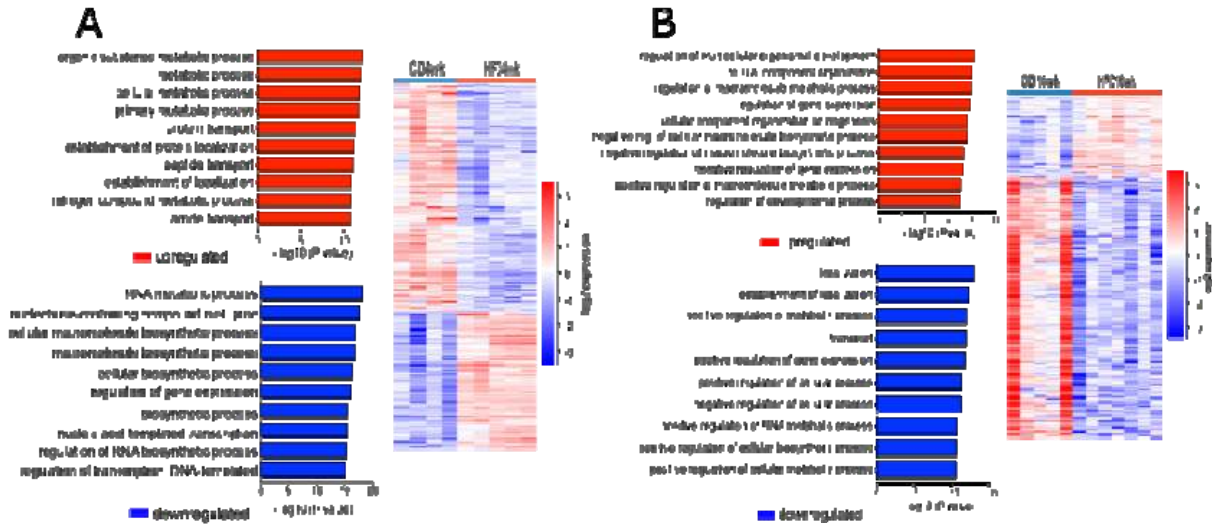
47 Immunohistochemical localisation of SOCS3 and PTP1B protein during follicle
48 development in mice fed chow diet (CD) or high fat diet (HFD) for 4 and 16 weeks
49 (wk) and intraperitoneally injected with saline (C) or leptin (L) for 16 days (d). Positive
50 staining in brown, counterstaining with heamatoxylin. Negative control stained with
51 polyclonal rabbit IgG (A, B) 4 wk CD, (C, D) 4 wk HFD, localisation in secondary
52 follicle SOCS3 (E) 4 wk CD and (F) 4 wk HFD, PTP1B (G) 4 wks CD, (H) 4 wks HFD,
53 antral follicles SOCS3 (I) 16 wk CD, (J) 16 wk HFD, PTP1B (K) 16 wk CD, (L) 16 wk
54 HFD, preovulatory follicle SOCS3 (M) 16 C, (N) 16 L, PTP1B (O) 16 C, (P) 16 L. The
55 scale bar represents 100µm. The specificity of SOCS3 staining was confirmed by
56 immunofluorescent localisation in *ob/ob* mice with genetic deficiency of leptin. Positive
57 staining in orange, nuclear counterstaining with DAPI in blue. (Q-R) negative control
58 16 wk CD performed with polyclonal rabbit IgG, SOCS3 localised in (S, T) secondary
59 follicle and (U,V) antral follicle from controls (*ob/ob*. +/+; S,U) and leptin deficient
60 ovaries (*ob/ob* -/-; T,V). Images are representatives of 3 biological replicates. Inserts in
61 left top corners are the amplifications of granulosa cells. Pictures are representatives of
62 3 biological replicates. The scale bar represents 20µm.

63

64

65 Figure supplement 4. Wołodko et al., 2019

66



67

68 **Figure supplement 4. Differentially expressed genes and associated pathways in**
69 **cumulus cells from diet- induced obesity protocol.**

70 DESeq2 analysis of transcriptome data in cumulus cells obtained from mice after 4 or
71 16 weeks (wk) of chow diet (CD) or high fat diet (HFD). N= 3-7 mice per group.

72 On the right heatmap showing hierarchical clustering of (A) 997 differentially expressed
73 genes after submitting mice to 4 weeks of CD and HFD, (B) 846 differentially
74 expressed genes after submitting mice to 16 weeks of CD and HFD. On the left
75 presentation of pathways of genes with the most significant enrichment after gene
76 ontology analysis. Gene ontology analysis performed with Gene Ontology Enrichment
77 Analysis and Visualisation Tool.

78

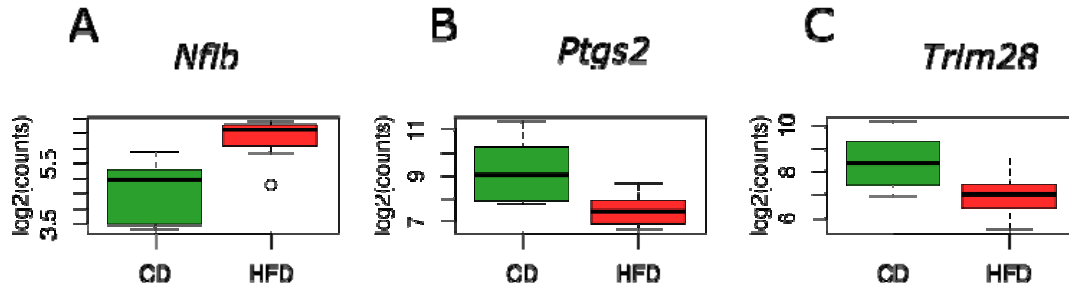
79

80

81 Figure supplement 5. Wołodko et al., 2019

82

83



84

85

86 **Figure supplement 5. Oocyte competence and embryo quality markers**
87 **differentially expressed in cumulus cells from mice with late obesity.**

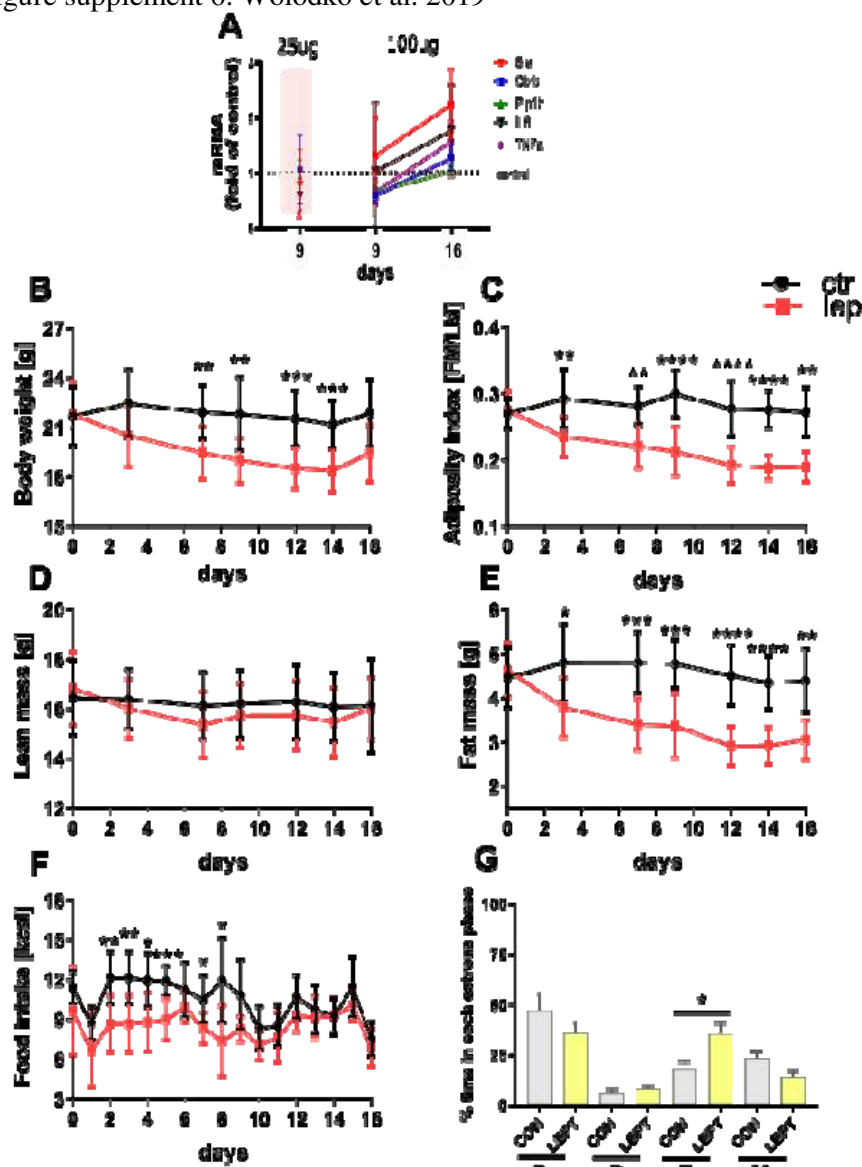
88 DESeq2 analysis of transcriptome data in cumulus cells obtained from mice after 16
89 weeks of chow diet (CD) or high fat diet (HFD). N= 3-7 mice per group.

90 Expression of embryo quality markers (A) *nuclear factor I B (Nfib)*, (B) *cyclooxygenase*
91 *2 (Ptgs2)* and oocyte competence marker (C) *tripartite motif containing 28 (Trim28)*.

92 Log₂ of counts.

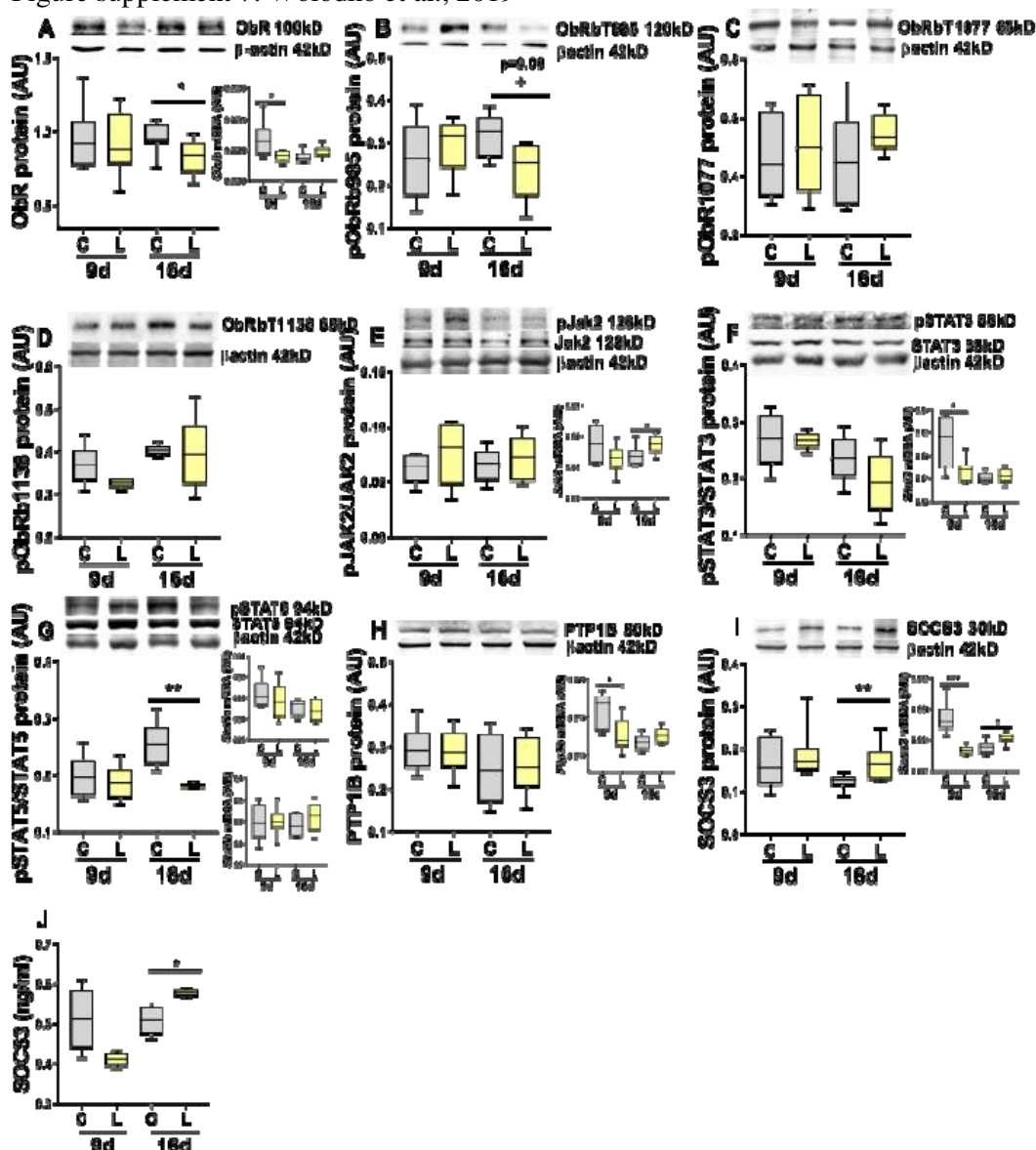
93

94



96
 97 **Figure supplement 6. Pharmacologically hyperleptinemic mouse model validation.**
 98 In order to validate the length of the treatment and the dose of leptin, we analysed whole
 99 ovary mRNA from animals treated with 25 or 100 µg of leptin for 9 or 16 d. Injection of
 100 100 µg for 16 days caused changes in the abundance of leptin-responsive transcripts
 101 (69–72) in ovarian extracts collected from animals in oestrous stage. Animals were
 102 injected with saline (C) or different doses of leptin (L) for 9 or 16 days (d). (A) mRNA
 103 level of *steroidogenic acute regulatory protein (Star)*, *long isoform of leptin receptor*
 104 *Obrb*, *protein tyrosine phosphatase non-receptor type 1 (Ptp1b)*, *interleukin 6 (Il6)*,
 105 *tumor necrosis factor a (Tnfa)* expressed as fold of control after injecting animals for 9
 106 or 16 days with 25µg or 100 µg of leptin. Changes in (B) body weight, (C) adiposity
 107 index, (D) lean mass, (E) fat mass, (F) food intake in mice intraperitoneally injected
 108 with saline (ctr, black line) or leptin (lep, red line) for 16 days. (G) Proportion of time
 109 spend in each oestrous phase of hyperleptinemic mice. D, dioestrus; E, oestrus; M,
 110 metoestrus; P, pro-oestrus. Each bar represents the mean ± SD. Differences in
 111 phenotype characteristics between groups were analysed by Mann-Whitney test,
 112 oestrous cycle distribution analysed by unpaired t-test. Data show mean values for
 113 n=10. * p<0.05; ** p<0.01; ***p<0.001
 114

115 Figure supplement 7. Wołodko et al., 2019



116

117

118

119

120

121

122

123

124

125

126

127

128

129

130

131

132

Figure supplement 7. Expression of leptin signalling components in the ovary of pharmacologically hyperleptinemic mice.

Abundance of mRNA (grey box) and protein of leptin signalling pathway components in ovarian extracts collected from animals injected with saline (C) or 100 μg of leptin (L) for 9 or 16 days (d) and sacrificed in oestrus stage. Expression of (A) leptin receptor (ObR), phosphorylation of (B) tyrosine 985 of leptin receptor, (C) tyrosine 1077 of leptin receptor, (D) tyrosine 1138 of leptin receptor, (E) Janus kinase 2 (JAK2), (F) signal transducer and activator of transcription 3 (STAT3), (G) STAT5, expression of (H) protein tyrosine phosphatase 1B (PTP1B) and (I) suppressor of cytokine signalling 3 (SOCS3) determined by real-time PCR and Western blot. (J) SOCS3 ovarian quantification in animals in oestrus stage determined by ELISA. mRNA expression of *Rpl37* and protein expression of β-actin was used to normalize the expression data. Each bar represents the mean ± SD. Differences between groups were analysed by Mann-Whitney test. N=4-8 for immunoblots and N=8 for RT PCR analysis and ELISA. * p<0.05; ** p<0.01; ***p<0.001; + p=0.09.

133 Figure supplement 8. Wołodko et al., 2019

134

135

136

137

138

139

140

141

142

143

144

145

146

147

148

149

150

151

152

153

154

155

156

157

158

159

160

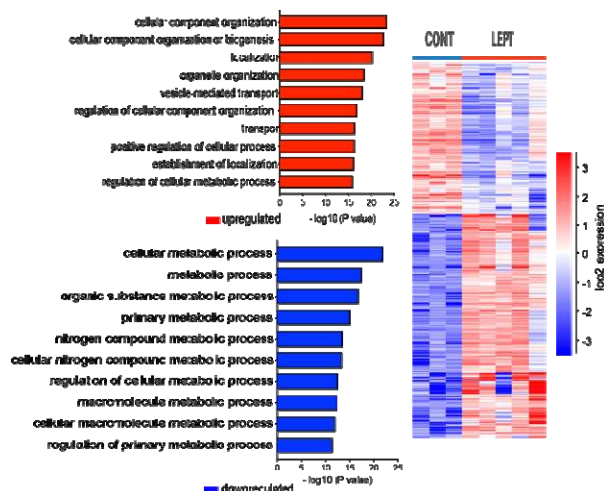
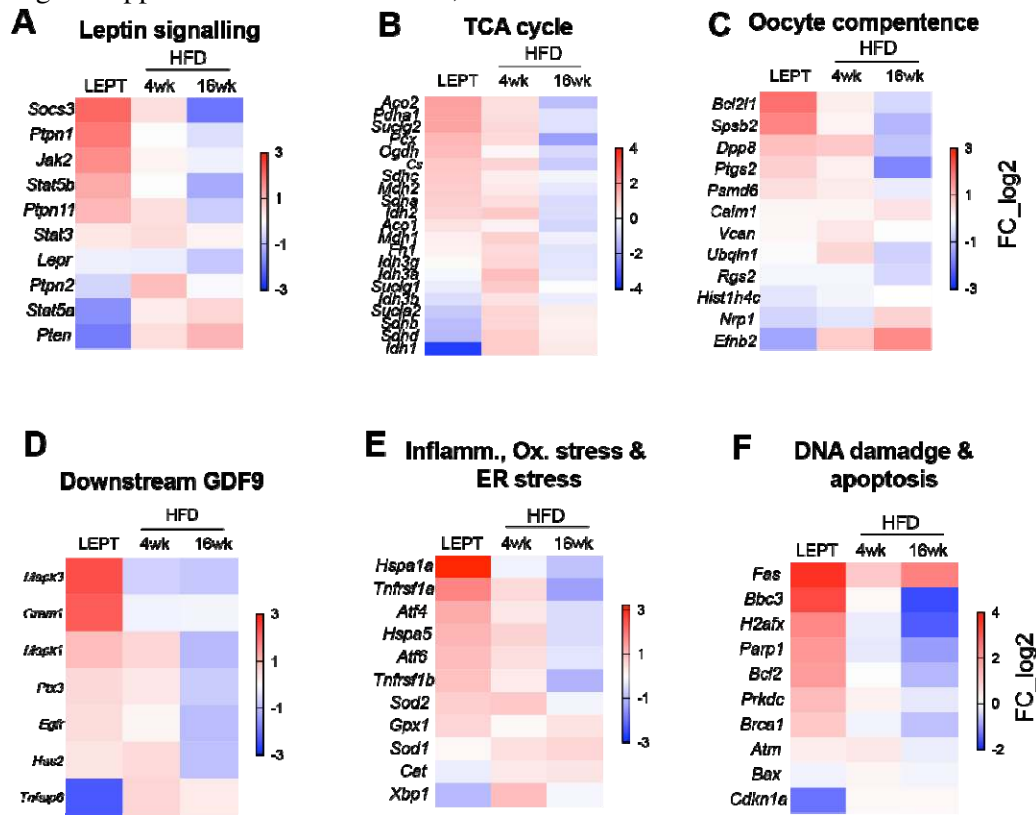


Figure supplement 8. Differentially expressed genes and associated pathways in cumulus cells from hyperleptinemic mice.

DESeq2 analysis of transcriptome data in cumulus cells obtained from mice treated with saline (CONT) and leptin (LEPT). N= 3-7 mice per group.

On the right heatmap showing hierarchical clustering of 2026 differentially expressed genes after treating mice with leptin for 16 days. On the left presentation of pathways of genes with the most significant relevance after gene ontology analysis. Gene ontology analysis performed with Gene Ontology Enrichment Analysis and Visualisation Tool.

161 Figure supplement 9. Wołodko et al., 2019



162

163

164 **Figure supplement 9. Similarities between profiles of genes differentially expressed**
 165 **in cumulus cells in diet induced- obese mice and leptin treated mice.**

166 DESeq2 analysis of transcriptome data in cumulus cells (CC) obtained from mice
 167 treated with saline (CONT) and leptin (LEPT) or after 4 or 16 weeks (wk) of chow diet
 168 (CD) or high fat diet (HFD). N= 3-7 mice per group. Heatmaps representing fold
 169 change in expression of genes associated with the following pathways or processes: (A)
 170 leptin signalling, (B) tricarboxylic acid (TCA) cycle, (C) oocyte competence, (D) genes
 171 regulated by oocyte-derived growth differentiation factor (GDF) 9, (E) inflammation,
 172 oxidative stress and endoplasmic reticulum stress, (F) DNA damage and apoptosis in
 173 CC. log₂_FC of reads per million (RPM)

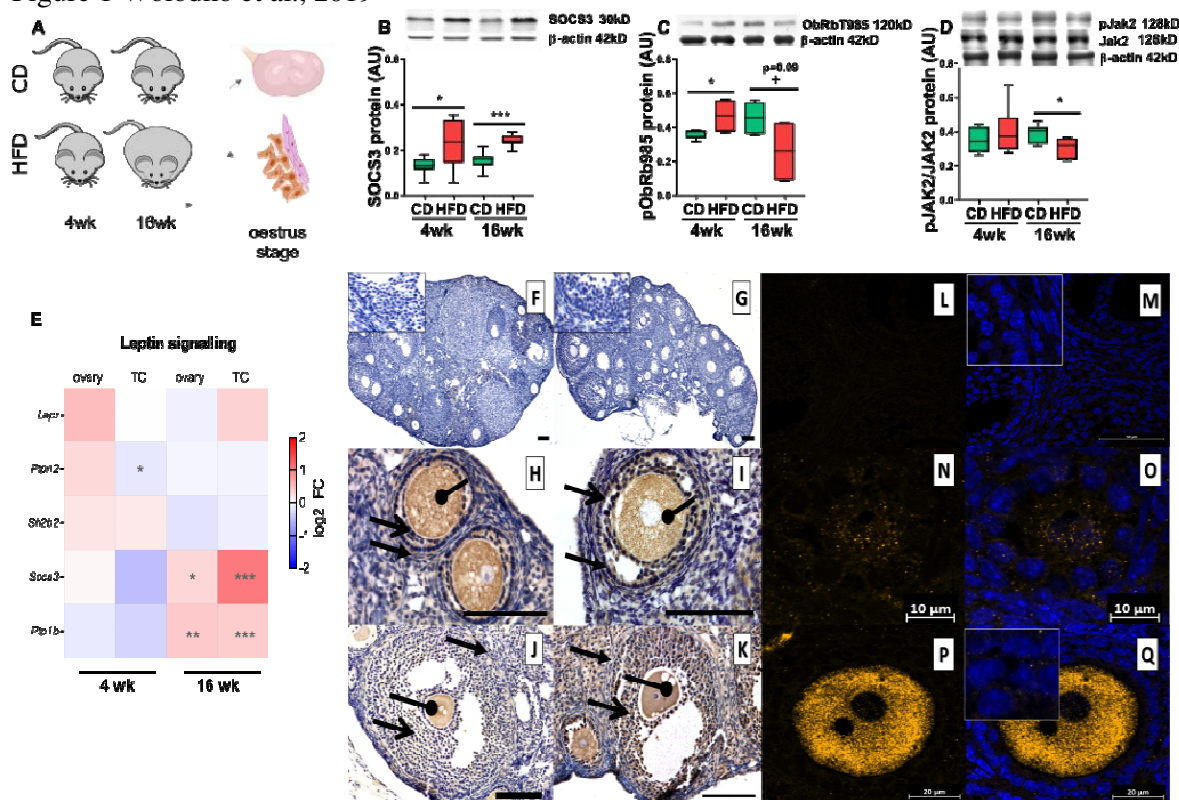
174

175

176

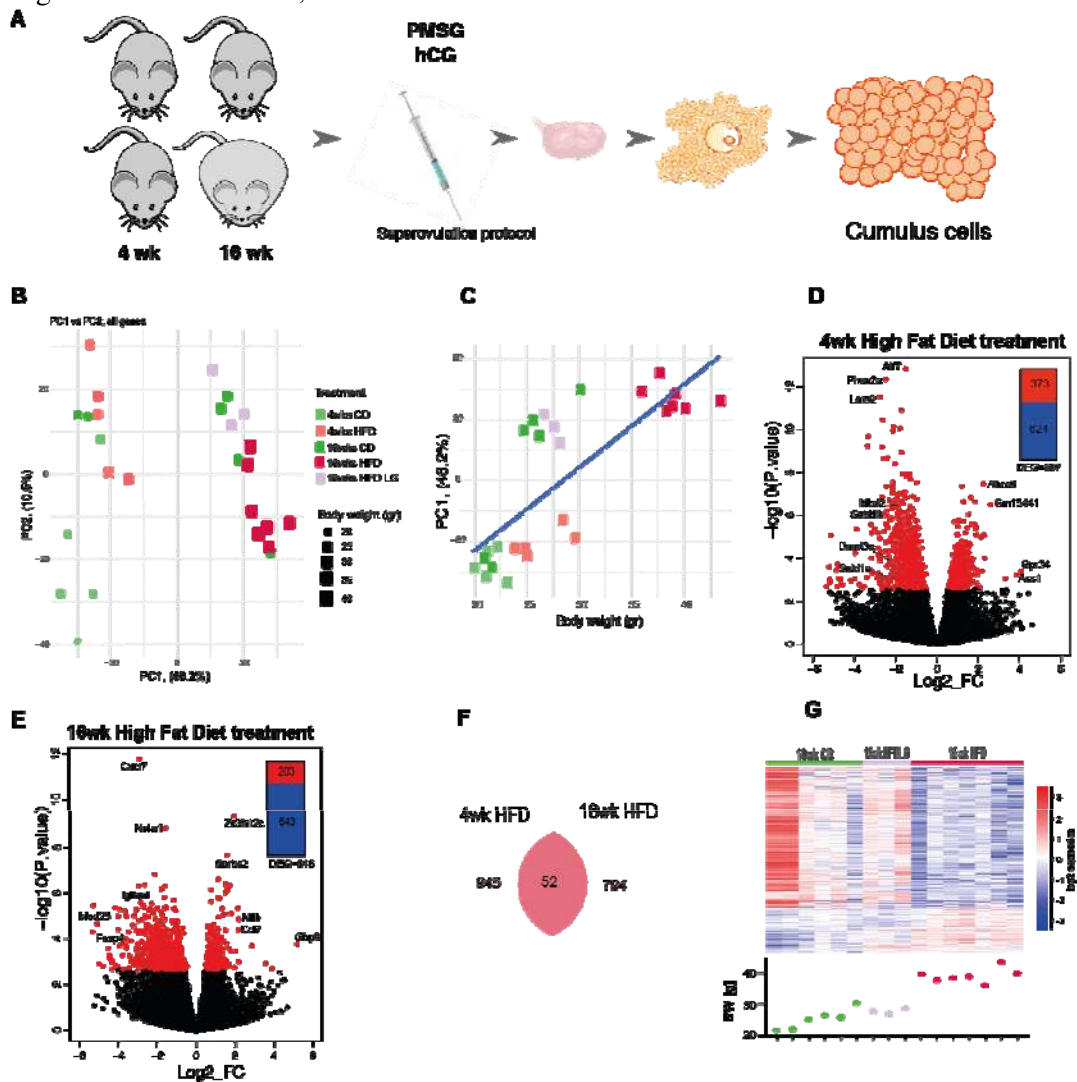
177

1 Figure 1 Wołodko et al., 2019



2
3
4
5
6
7
8
9
10
11
12
13
14
15
16
17
18
19
20
21
22
23
24
25
26
27
28

29 Figure 2 Wołodko et al., 2019

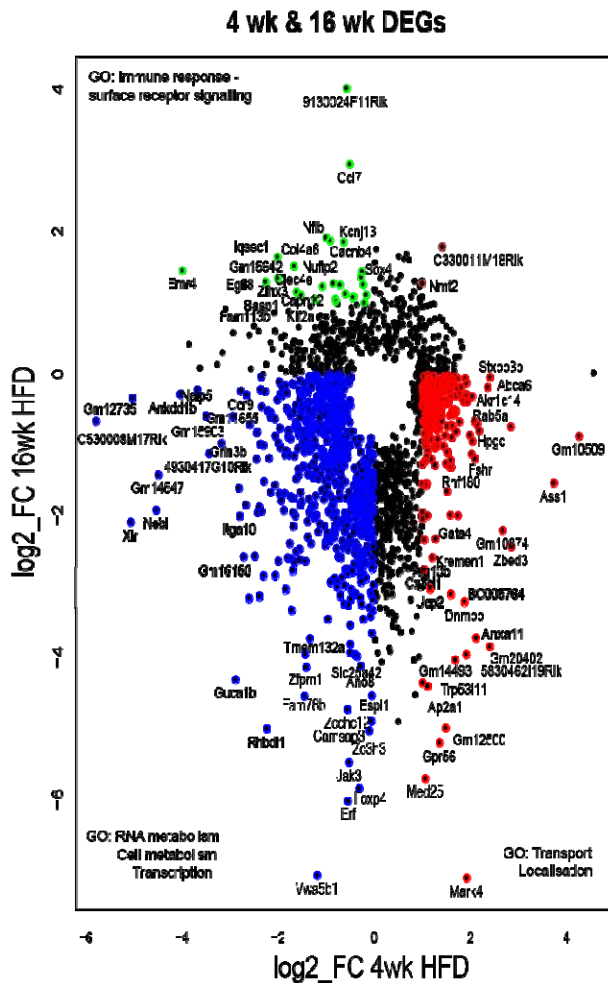


30
 31 **Figure 2. Cumulus cell transcriptome analysis in diet induced-obese mice reveals**
 32 **strong correlation with body weight.**

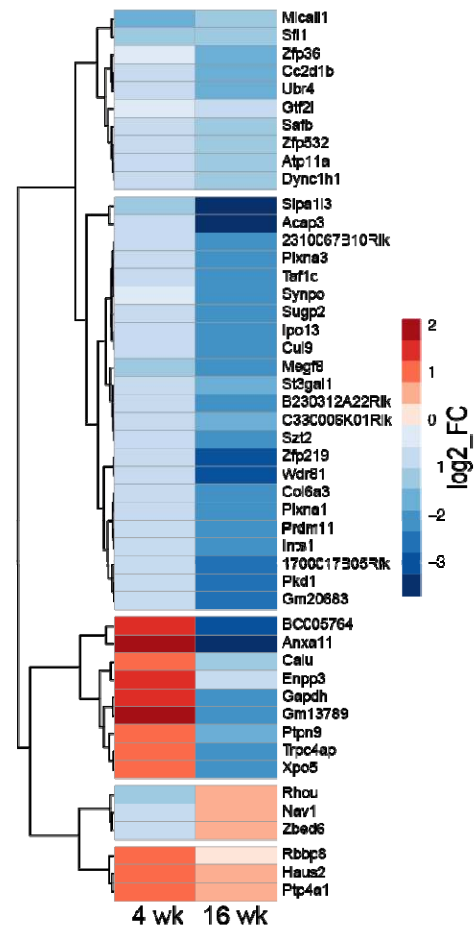
33 (A) Experimental design: mice were subjected to the indicated dietary protocol,
 34 superovulated and cumulus cells were collected from cumulus-oophorus-complexes.
 35 RNA-seq analysis of gene expression in cumulus cells obtained from mice after 4 or 16
 36 weeks (wk) on chow diet (CD), high fat diet (HFD) or low gainers on HFD (HFDLG).
 37 N= 3-7 mice per group. (B) Principal component analysis of global transcriptome shows
 38 samples cluster into 2 groups accordingly to their body weight (BW). (C) Correlation of
 39 Principal Component 1 (PC1) with BW; $r=0.777$, $p=3.026e-06$. Volcano plots showing
 40 distribution of differentially expressed genes in (D) 4wks HFD and (E) 16wks HFD;
 41 genes with False Discovery Rate <0.05 coloured red. (F) Venn diagram showing the
 42 number of genes differentially expressed at false discovery rate (FDR) <0.05 between 4
 43 wk and 16 wk groups. (G) Heatmap of 846 DEGs identified by DESeq2 analysis
 44 between 16wk CD and HFD CCs, including data for HFDLG CC samples, with BW of
 45 mice at time of collection plotted below. Heatmap representing fold of change of gene
 46 expression. \log_2_FC of reads per million (RPM).
 47

48 Figure 3 Wołodko et al., 2019

A



B

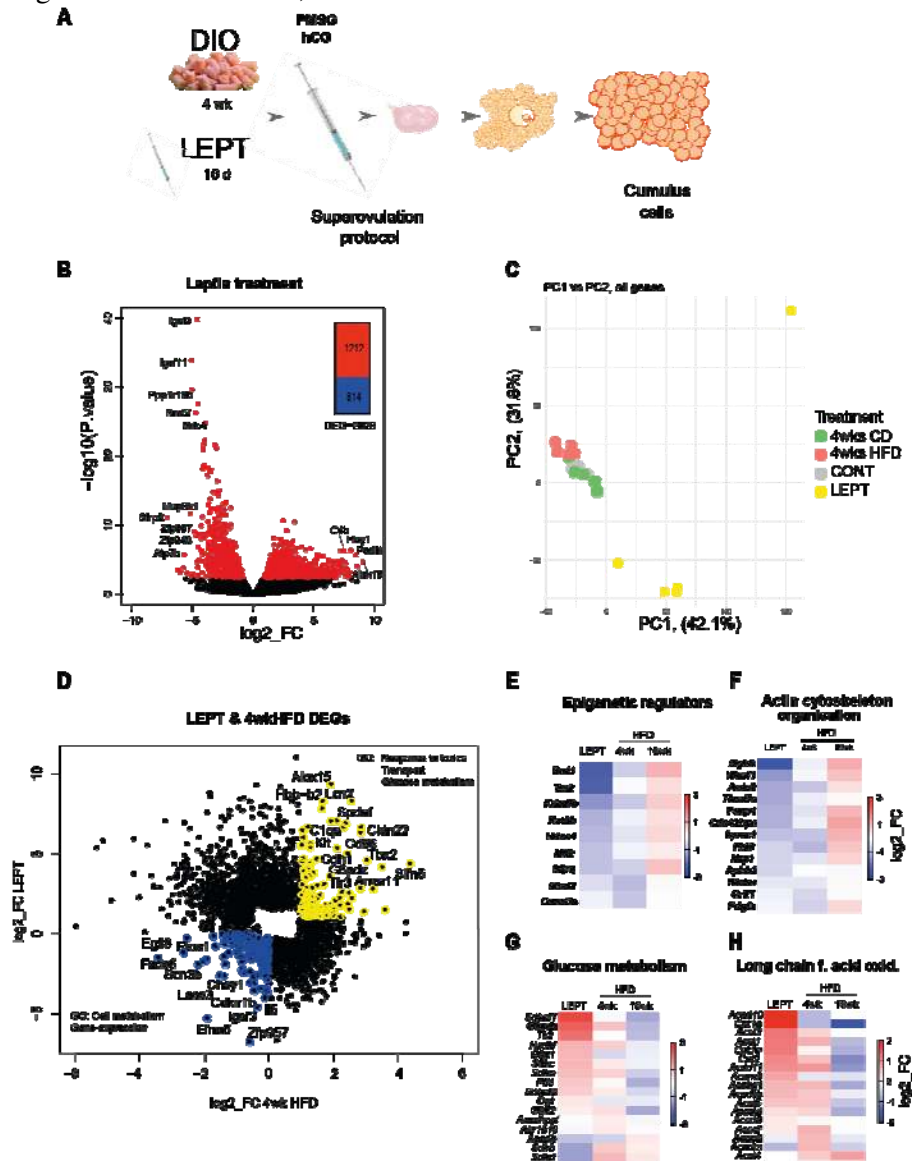


49

50 **Figure 3. Temporal changes in the transcriptome of cumulus cells during obesity**
 51 **progression.**

52 DESeq2 analysis of transcriptome data in cumulus cells (CC) of mice fed high fat diet
 53 (HFD) for 4 or 16 weeks (wk). N= 3-7 mice per group. (A) Scatter plot presents genes
 54 differentially expressed in at least one condition (False Discovery Rate <0.05) in CC
 55 after 4 wk (997 genes) or 16 wk HFD (846 genes). Genes coloured blue are
 56 downregulated after both 4wk and 16wk HFD; green downregulated after 4 wk HFD
 57 and upregulated after 16wk HFD; brown upregulated after both 4 wk HFD and after
 58 16wk; red upregulated after 4 wk HFD and downregulated after 16 wk HFD. (B)
 59 Heatmap presents hierarchical clustering of genes significantly changed in both 4 and
 60 16 wk HFD normalised by average control fed chow diet. Genes cluster in group
 61 downregulated after 4 wk and 16 wk HFD, group upregulated after 4 wk and
 62 downregulated after 16 wk HFD, group downregulated after 4 wk and upregulated after
 63 16wk HFD and group upregulated after both 4 wk and 16 wk HFD. Gene ontology
 64 analysis performed with Gene Ontology Enrichment Analysis and Visualisation Tool.
 65 log₂_FC of reads per million (RPM).
 66

67 Figure 4 Wołodko et al., 2019

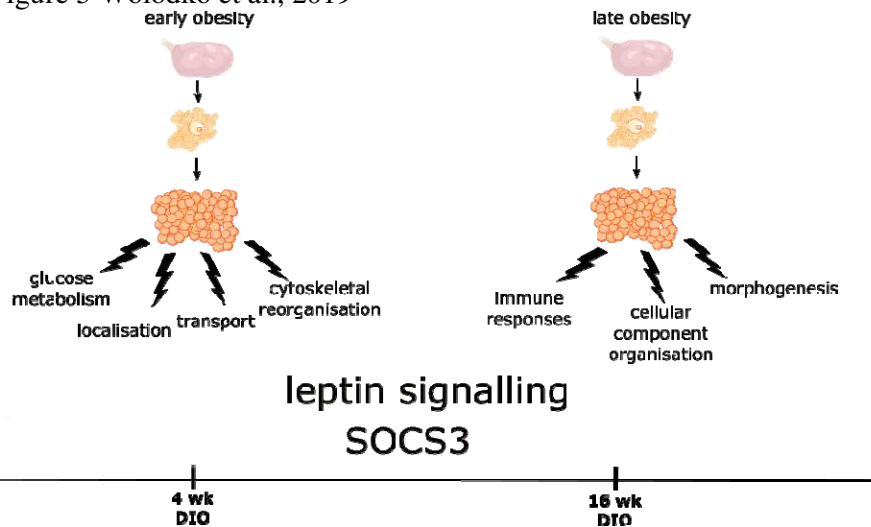


68

69 **Figure 4. Pharmacologically hyperleptinemic mouse model shows leptin effects in**
 70 **the transcriptome of cumulus cells during early obesity .**

71 (A) Experimental design: mice were fed chow diet (CD) or high fat diet (HFD) for 4
 72 weeks (wk) (4 wk DIO) or injected with saline (CONT) or 100µg of leptin (LEPT) for
 73 16 days, followed by superovulation and collection of cumulus cells from cumulus-
 74 oophorus-complexes. RNA-seq analysis of gene expression in cumulus cells. N=3-7
 75 mice per group. (B) Volcano plots showing distribution of differentially expressed
 76 genes in LEPT group; genes with False Discovery Rate <0.05 coloured red. (C)
 77 Principal component analysis of global transcriptome shows LEPT effect is the main
 78 source of variance in the data (first principal component, PC1). DESeq2 analysis of
 79 transcriptome data in cumulus cells. (D) Scatter plot presents genes differentially
 80 expressed in cumulus cells in LEPT or in 4 wk HFD, with False Discovery Rate <0.05.
 81 Those coloured blue are down-regulated both in response to leptin treatment and 4 wk
 82 HFD; those in yellow upregulated by both treatments. Heatmaps presenting fold of
 83 change in expression of genes associated with the following pathways: (E) epigenetic
 84 regulation; (F) actin cytoskeleton organisation; (G) glucose metabolism; (H) long chain
 85 fatty acid oxidation in CC. Gene ontology analysis performed with Gene Ontology
 86 Enrichment Analysis and Visualisation Tool. log₂_FC of reads per million (RPM)

87 Figure 5 Wołodko et al., 2019



88

89 **Figure 5. Graphical representation of the main temporal changes in the ovary of**
90 **obese mice.**

91 During early obesity (4 weeks of diet-induced obesity, DIO) increased leptin signalling
92 affects the transcriptome of cumulus cells (CCs). RNA-seq analysis revealed mainly
93 alterations in genes involved in membrane trafficking, cytoskeleton organisation and
94 glucose metabolism. During late obesity (16 wk DIO) leptin resistance is established,
95 which causes accumulation of SOCS3 in the ovary. Transcriptome analysis of CCs at
96 this timepoint indicated the activation of the inflammatory response and cellular
97 anatomical morphogenesis, with inhibition of metabolism and transport.

98

99